Leptin-dependent differential remodeling of visceral and pericardial adipose tissue following chronic exercise and psychosocial stress

Received: 14 February 2023 | Revised: 6 November 2023 | Accepted: 8 November 2023

DOI: 10.1096/fj.202300269RRR

RESEARCH ARTICLE

The FASEB Journal

Leptin-dependent differential remodeling of visceral and pericardial adipose tissue following chronic exercise and psychosocial stress

Susan Ige[1] | **Kaouthar Alaoui**[1] | **Alaa Al-Dibouni**[1] | **Mark L. Dallas**[1] | **Felino R. Cagampang**[2] | **Dyan Sellayah**[1] | **Paul D. Chantler**[3] | **Samuel Y. Boateng**[1]

[1]Institute of Cardiovascular and Metabolic Research, School of Biological Sciences, University of Reading, Reading, UK

[2]Institute of Developmental Sciences, Human Development and Health, Faculty of Medicine, University of Southampton, Southampton, UK

[3]School of Medicine, West Virginia University, Morgantown, West Virginia, USA

Correspondence
Samuel Y. Boateng, Institute of Cardiovascular and Metabolic Research, School of Biological Sciences, Health, and Life Sciences Building, University of Reading, Whiteknights, Reading, Berkshire RG6 6UB, UK.
Email: s.boateng@reading.ac.uk

Funding information
NIH, NINDS BINP RO1, Grant/Award Number: NS117754; Petroleum Technology Development Fund, Abuja, Nigeria

Abstract

Obesity is driven by an imbalance between caloric intake and energy expenditure, causing excessive storage of triglycerides in adipose tissue at different sites around the body. Increased visceral adipose tissue (VAT) is associated with diabetes, while pericardial adipose tissue (PAT) is associated with cardiac pathology. Adipose tissue can expand either through cellular hypertrophy or hyperplasia, with the former correlating with decreased metabolic health in obesity. The aim of this study was to determine how VAT and PAT remodel in response to obesity, stress, and exercise. Here we have used the male obese Zucker rats, which carries two recessive *fa* alleles that result in the development of hyperphagia with reduced energy expenditure, resulting in morbid obesity and leptin resistance. At 9 weeks of age, a group of lean (*Fa/Fa* or *Fa/fa*) Zucker rats (LZR) and obese (*fa/fa*) Zucker rats (OZR) were treated with unpredictable chronic mild stress or exercise for 8 weeks. To determine the phenotype for PAT and VAT, tissue cellularity and gene expression were analyzed. Finally, leptin signaling was investigated further using cultured 3T3-derived adipocytes. Tissue cellularity was determined following hematoxylin and eosin (H&E) staining, while qPCR was used to examine gene expression. PAT adipocytes were significantly smaller than those from VAT and had a more beige-like appearance in both LZR and OZR. In the OZR group, VAT adipocyte cell size increased significantly compared with LZR, while PAT showed no difference. Exercise and stress resulted in a significant reduction

Abbreviations: AdipoQ, adiponectin; CAD, coronary artery disease; CANX, calnexin; CAV, caveolin-1; CT, computed tomography; CTGF, connective tissue growth factor; DMSO, dimethyl sulfoxide; EAT, epicardial adipose tissue; EMRI, EGF-like module-containing mucin-like hormone receptor-like 1; ER, endoplasmic reticulum; Ex, exercise; FABP4, fatty acid binding protein 4; H&E, haematoxylin and Eosin; HEX, 1,2,3,4,5,6-hexabromocyclohexane; HPA, hypothalamic-pituitary-adrenal; HSD11B1, 11β-hydroxysteroid dehydrogenase type 1; IBMX, 3-isobutyl-1-methylxanthine; IRS1, insulin receptor substrate 1; JAK2, Janus kinase 2; LEP, leptin; LZR, lean Zucker rat; NIH, National Institute of HEALTH; OCT, optimal cutting temperature; OZR, obese Zucker rats; PAT, pericardial adipose tissue; PGC1α, peroxisome proliferator-activated receptor-gamma coactivator-1 alpha; POSTN, periostin; PPARγ, peroxisome proliferator activated receptor gamma; PPIA, peptidylprolyl isomerase A; TIMP, tissue inhibitor of metalloprotease; TNFα, tumour necrosis factor alpha; UCMS, unpredictable chronic moderate stress; UCP1, uncoupling protein 1; VAT, visceral adipose tissue; WVUHSC, West Virginia University Health Science Centre.

in VAT cellularity in OZR, while PAT showed no change. This suggests that PAT cellularity does not remodel significantly compared with VAT. These data indicate that the extracellular matrix of PAT is able to remodel more readily than in VAT. In the LZR group, exercise increased insulin receptor substrate 1 (IRS1) in PAT but was decreased in the OZR group. In VAT, exercise decreased IRS1 in LZR, while increasing it in OZR. This suggests that in obesity, VAT is more responsive to exercise and subsequently becomes less insulin resistant compared with PAT. Stress increased PPAR-γ expression in the VAT but decreased it in the PAT in the OZR group. This suggests that in obesity, stress increases adipogenesis more significantly in the VAT compared with PAT. To understand the role of leptin signaling in adipose tissue remodeling mechanistically, JAK2 autophosphorylation was inhibited using 5 μM 1,2,3,4,5,6-hexabromocyclohexane (Hex) in cultured 3T3-derived adipocytes. Palmitate treatment was used to induce cellular hypertrophy. Hex blocked adipocyte hypertrophy in response to palmitate treatment but not the increase in lipid droplet size. These data suggest that leptin signaling is necessary for adipocyte cell remodeling, and its absence induces whitening. Taken together, our data suggest that leptin signaling is necessary for adipocyte remodeling in response to obesity, exercise, and psychosocial stress.

1 | INTRODUCTION

Exposure to chronic psychosocial stress with sustained hyperactivity of the endocrine stress system has been implicated in visceral obesity,[1] insulin resistance,[2] and the development of diabetes mellitus.[3] The visceral adipose tissue (VAT) involved in these metabolic pathologies is those which surround the abdominal organs, particularly the perigonadal region, as well as the retroperitoneal fat pads located on the kidneys, and the mesenteric fat pad located alongside the intestinal tract. In response to chronic psychosocial stress, the persistent release of cortisol leads to overeating, reduced lipid mobilization, increased adipocyte differentiation, and obesity despite high circulating leptin concentrations.[4,5] However, the visceral fat depot around the heart has not been studied in detail. This fat depot is referred to as pericardial adipose tissue (PAT). PAT is distinct from epicardial adipose (EAT) in that it does not make physical contact with the heart muscle but is separated by the pericardial sac. Little is known about the impact of chronic psychosocial stress on PAT phenotype. Computed tomography (CT) scanning showing the presence of PAT in humans shows an increased volume in response to a poor diet,[6] as well as in patients with type 2 diabetes mellitus.[7] It has been suggested that the mechanical effects of increased PAT thickness may limit the distensibility of the heart even in healthy subjects with normal cardiac function and could contribute to diastolic dysfunction.[8] It was demonstrated in obese minipigs that PAT exhibits a different fatty acid profile[9] and a higher level of inflammatory adipokines including leptin and lipid peroxides than VAT which are all associated with the severity of myocardial fibrosis.[10] Therefore, excessive amounts of PAT may have a direct impact and modulate the structure, as well as the function, of the adjacent myocardium through paracrine signaling.[11,12]

Specifically, the change in adipokine profiles from anti-inflammatory to proinflammatory adipokines influences cardiac function.[13] Studies have reported a strong relationship between PAT volumes with the incidence of coronary artery disease,[14,15] however, little is known about the adipokines produced by PAT in clinical settings. A study reported that PAT from the patients with chronic valvular heart disease expressed high levels of uncoupling protein 1 (UCP1) which is mainly expressed in brown adipose tissue, and acts in thermogenesis, the regulation of energy expenditure, but is markedly reduced in PAT from patients with coronary artery disease.[16] In addition, the transcriptome of PAT from patients with CAD revealed an upregulation of genes involved in immune and inflammatory processes.[14,17]

Exercise training has shown numerous beneficial effects on adipose tissue health in rodents[18] and humans.[19] In well-conditioned athletes, the mass of adipose tissue accounts for 2% to 3% of body weight, suggesting the beneficial role of exercise in reducing fat mass.[20] A clinical study demonstrated that aerobic exercise significantly reduced the total body fat mass and increased muscle mass in overweight women after 12 weeks of training.[21] Some other studies from rodents demonstrated that exercise

training increased mitochondrial biogenesis in visceral[22] and subcutaneous adipose tissue.[23]

The beneficial effects of exercise training are not limited to weight loss and maintenance, but their positive impact on reducing the symptoms and risk of depression and anxiety has also been documented in humans.[24,25] However, the mechanisms behind the effects of exercise on physiological adaptation to psychosocial stress are limited. It has been reported that the physiological adaptation to exercise and psychosocial stress shares the similarities of hyperactivity of the hypothalamic–pituitary–adrenal axis.[26] In this study, we investigated the differential effects of obesity, exercise training, and chronic psychosocial stress on the VAT and PAT phenotype in obese Zucker rats to determine the potential role of leptin signaling.

2 | MATERIALS AND METHODS

2.1 | Animal study

The aerobic exercise training and unpredictable chronic mild stress protocols were performed in the animal care facility at the West Virginia University Health Science Centre (WVUHSC), United States of America. It was approved by the WVUHSC Animal Care and Use Committee, which follows the National Institutes of Health (NIH) Guide for the Care and Use of Laboratory Animals as reported in the previous publication.[27] Male lean (LZR) and obese (OZR) rats of the Zucker strain aged 16–17 weeks were used for this study. At 8–9 weeks of age, LZR and OZR were divided into four separate experimental groups with at least 14 rats per group: (1) age-matched controls; (2) unpredictable chronic mild stress (UCMS); (3) treadmill exercise (Ex); or (4) UCMS with treadmill exercise (UCMS/Exercise). VAT and PAT tissues were collected at the end of the experiment and stored at -80°C prior to use.

2.1.1 | UCMS protocol

The UCMS protocol is a well-defined model to induce a depressive state in rodents.[28] Rodents undergoing UCMS manifest with clinically relevant depressive symptoms such as anhedonia and learned helplessness[28] with alterations in brain structure and function parallel to clinical depression.[29] Rats were singly housed in UCMS groups and exposed to the following mild environmental stressors in randomly chosen sequences for 8 h each day, 5 days/week, over the course of 8 weeks: *Damp bedding*—10 oz. of water was added to each standard cage, *bath*—all bedding was removed and ~0.5 inches of water was added to empty cage, water temperature was room temperature, ~24°C, *cage Tilt*—cage was tilted to 45 degrees without bedding, *social stress*—each rat was switched into a cage of a neighboring rat, *no bedding*—all bedding was removed from the cage, *alteration of light/dark cycles*—turning lights off/on in random increments for scheduled period.

2.1.2 | UCMS and exercise combination protocol

LZR UCMS/Ex and OZR UCMS/Ex underwent 8 weeks of treadmill running. Animals ran 5 days/week in individual lanes on a motor-driven treadmill at a 5% grade. During the first week, animals were acclimatized to the treadmill by progressively increasing running time form 20 min until a duration of 60 min was achieved. A maximum speed test was then performed on each animal and target running speed was set for 60%–70% of that maximum. Workouts for the following 7 weeks were 60 min in duration and consisted of 15 min of gradual increases in speed until reaching target speed, which was maintained for remaining 45 min. Mild electrical stimulation was used to encourage running. Treadmill running was performed first thing in the morning immediately followed by subjection to the UCMS protocol as described above.

2.1.3 | Coat score

The rodents' coat scores were evaluated throughout the duration of the 8-wk protocol. Each week, the rats were weighed and inspected for grooming habits. The total cumulative coat score was computed by giving an individual score of 0 (clean) or 1 (dirty) to eight different body parts (i.e., the head, neck, back, forelimbs, stomach, hind limbs, tail, and genitals).

2.1.4 | Terminal procedures

Terminal procedures were performed a minimum of 48 h following the last bout of Ex or UCMS to eliminate the acute effects of Ex or UCMS on experiments. At time of terminal procedures, animals were weighed then deeply anesthetized with pentobarbital sodium (50 mg/kg ip). All rats then received carotid artery and jugular vein cannulation to measure mean arterial pressure.

2.1.5 | Circulating cortisol

Corticosterone is a glucocorticoid produced by the adrenal cortex in response to corticotropic hormone and is the

precursor to aldosterone. Corticosterone is the main glucocorticoid in rodents because cortisol is in humans. The production of glucocorticoids is increased by stress. Using a commercially available enzyme-linked immunosorbent assay kit (Cayman Chemical, item no. 501320) serum samples, collected at the time of terminal surgery, were examined for corticosterone levels in duplicate according to the manufacturer's instructions.

2.2 | Histological analysis

The isolated VAT and PAT were embedded in Optimal Cutting Temperature (OCT) media and sectioned at 13 μm thickness using Bright cryostat at −33°C and −35°C for specimen and chamber temperatures, respectively. Sections were stained with Hematoxylin and Eosin (H&E) to quantify adipocyte cellularity. To evaluate total extracellular matrix deposition, we performed picrosirius red staining of collagen fibrils on VAT and PAT sections from LZR and OZR using Picrosirius Red (PSR) staining kit (ab150681, Abcam). The distinct architecture of adipose tissue allows the visualization of the collagen accumulation in the interstitial space and pericellular matrix when sections were visualized using a Nikon TE200 Brightfield Inverted Microscope at 10× objective lens. As previously described (Hadi et al., 2011), the quantification of the images was carried out using Image J software by converting the image into greyscale before using the "Threshold" tool on ImageJ. Using Image>Type>RGB Stack command, the RGB image produced by PSR was deconvoluted into separate channels. The "Threshold" tool detected the fibrosis and automatically highlighted the PSR-stained collagen in red. The channel with the best image quality was selected for the quantification. Moreover, the scale bar and other artifacts were removed from each image using the color picker tool (Image>Color>Color Picker) to exclude them from being included in the calculated area. The total fibrosis for each image was expressed as the percentage ratio of the signal intensity from the picrosirius red staining to the area of the total adipocytes (i.e., area of fibrosis / (area of adipocytes + area of fibrosis)×100).

2.3 | RNA isolation and RT-qPCR analysis

As previously described,[30] frozen VAT and PAT samples were homogenized in Invitrogen™ TRI Reagent™ solution (1 mL of TriZol for ≤200 mg of tissue) to extract RNA. The RNA isolation was performed according to manufacturer instructions packed with Invitrogen™ TRI Reagent™ Solution (Fisher Scientific). The quality of the purified RNA was prepared according to the Agilent RNA 6000 Nano Kit quick start guide (Cat# 5067-1511) and assessed on the Agilent 2100 bioanalyzer. The total RNA was reversely transcribed using the Applied Biosystems™ High-Capacity cDNA Reverse Transcription Kit (Fisher Scientific) and Invitrogen™ RNaseOUT™ Recombinant Ribonuclease Inhibitor (Fisher Scientific) according to manufacturer instructions, performed using the T100™ Thermal cycler (Bio-Rad). The mRNA abundance was measured by RT-qPCR using TaqMan Assays and 2x qPCRBIO Probe Mix No-ROX (PCR Biosystems, UK). Real-time quantitative PCR was performed in 20 μL reaction mixtures by pipetting 5 μL of diluted cDNA into all 96 wells (depending on the number of samples) in duplicate and 15 μL probe mix was added into the duplicate wells. The plate was sealed with optical film and centrifuged for 2 min at 2500 rpm to get all liquids to the bottom of the wells. The reaction was performed with a sequence detection system (MyiQ™ Bio-Rad UK) as follows: 95°C for 2 min, 95°C for 5 s (40 cycles of denaturation), and 60°C for 25 s (annealing/extension). The list of primers (TaqMan™ Gene Expression Assay (FAM-MGB) were purchased from Fisher Scientific (Table 1).

2.4 | Differentiation and culture adipocytes

3T3-l1 preadipocytes were induced to differentiate into mature adipocytes, and cells were treated with a base media composed of high glucose Dulbecco modified eagle medium (4500 mg/mL), 10% fetal bovine serum and 100 I.U./ml penicillin–streptomycin, which we refer to as DMEM10. The induction of adipogenesis was achieved when the cells were exposed to 0.5 mM 3-Isobutyl-1-methylxanthine (IBMX), 10 mM dexamethasone, and 10ug/mL insulin. 72 h later, cells were then treated with both DMEM10 and insulin10ug/mL for the remaining 6 days of the culture, cells were maintained in DMEM10 only, with the media being refreshed every 78 h. The whole adipogenesis experiment lasted for a total of 10 days at 37°C in 5% CO_2.

2.5 | Inhibition of JAK2 signaling through the addition of Hex

Once the adipocytes were fully mature, the addition of 5 μM Hex was used to inhibit JAK2 signaling. A 9 mM Hex stock was prepared by dissolving Hex in DMSO, a 5 μM hex working solution was generated in DMEM10. The adipocytes were maintained in Hex for an additional 48 h at 37°C in 5% CO_2 before analysis.

TABLE 1 Details of the TaqMan® probes used for real-time PCR assays.

Gene	Order number		Amplicon length (bp)	Probe context sequence
	ID	Catalogue		
PPIA	Rn00690933_m1	4331182	149	TCATGTGCCAGGGTGGTGACTTCAC
PPARG	Rn00440945_m1	4331182	105	TCTCAGTGGAGACCGCCCAGGCTTG
PGC1A	Rn00580241_m1	4331182	94	TGGAACTGCAGGCCTAACTCCTCCC
UCP1	Rn00562126_m1	4331182	69	CTCTTCAGGGAGAGAAACGCCTGCC
FABP4	Rn00670361_m1	4331182	69	AGGAAAGTGAAGAGCATCATAACCC
CANX	Rn01459976_m1	4331182	84	GGCTGCAGAGCCAGGTGTAGTGGGG
IRS1	Rn02132493_s1	4331182	147	AGAGACATGAGCGATCCCTTCAAGT
HSD11B1	Rn00567167_m1	4331182	80	TCTCCTCCATGGCTGGGAAAATGAC
CAV1	Rn00755834_m1	4331182	64	CGACGACGTGGTCAAGATTGACTTT
TNFA	Rn99999017_m1	4331182	108	ACCCTCACACTCAGATCATCTTCTC
ADIPOQ	Rn00595250_m1	4331182	63	GGGAGACGCAGGTGTTCTTGGTCCT
LEP	Rn00565158_m1	4331182	92	TTTCACACACGCAGTCGGTATCCGC
EMR1	Rn01527631_m1	4331182	100	CTGTCTGCTCAACCGCCAGGTACGA
CTGF	Rn01537277_g1	4331182	56	GATTGGCGTGTGCACTGCCAAAGAT
POSTN	Rn01494627_m1	4331182	78	AAGGCTGCCCAGCAGTGATGCCCAT
TIMP3	Rn00441826_m1	4331182	59	CTCCGACATCGTGATCCGGGCCAAA

2.6 | Palmitate treatment to generate hypertrophic adipocytes

After the full 10 days of adipogenesis, mature adipocytes were treated with 500uM palmitate diluted in 0.25% bovine serum Dulbecco modified eagle medium for an additional 48 h. The preparation of the palmitate stock was done as follows: Sodium palmitate was sonicated in a heated water bath in pure ethanol. The stock was heated up to 60 degrees to allow the palmitate to melt, in 0.25% bovine serum Dulbecco modified eagle medium, 50uL of the palmitate stock was added. The mix was heated to 30 degrees prior to being added to the cells. To investigate the effects of JAK2 inhibition on adipocyte hypertrophy, adipocytes were incubated in Hex alone for 2 h prior to the addition of palmitate and hex for an additional 48 h at 37°C in 5% CO_2.

2.7 | Adipocyte and lipid droplet surface area quantification

Brightfield images were captured using the NikonTi2 epifluorescent microscope at 40× magnification. Using the Java-based image processing program ImageJ, both adipocyte and lipid droplet area was manually quantified to be further analyzed.

2.8 | Data analysis

Data analysis was performed using GraphPad Prism software. Normality was evaluated by the Shapiro–Wilk normality test. All data are expressed as mean ± SEM. Differences between LZR and OZR were assessed using an unpaired *t*-test to determine differences between the groups for parametric data. Non-parametric data were assessed using Mann–Whitney *U* test to determine differences between the groups. The effects of the experimental interventions were determined with one-way ANOVA (i.e., Control vs. UCMS, Ex and UCMS/Ex). Non-parametric data were assessed using Kruskal–Wallis' test, followed by Dunn's multiple comparison test to determine the effects of the experimental interventions. The size distribution was analyzed using two-way ANOVA followed by Bonferroni post hoc test to the differences. Results were considered significant when $p < .05$.

3 | RESULTS

3.1 | Impaired metabolic profiles in obese Zucker rats

Various physiological measurements were taken from the animals used in this study following the various

treatments. These are shown in Table 2. At the end of the treatment period, the body weight (BW) of the OZR was about 25% ($p < .0001$) higher than LZR. Irrespective of their experimental conditions. In response to UCMS treatment, exercise ($p < .01$) and UCMS/exercise ($p < .05$), there was a significant weight loss across the experimental group in LZR. The body weight of OZR also decreased in response to UCMS ($p < .001$), and UCMS/exercise ($p < .0001$). However, there was no significant change observed in the body weight of the OZR when compared to the control group following 8 weeks of exercise training. The effects of the various physiological treatments and their impact on body weight can be seen over the 8-week treatment period (Figure S1A–C).

Compared to LZR, OZR developed hyperinsulinemia and hyperglycemia when biological parameters were measured in the blood. While UCMS, exercise, and UCMS/exercise had no significant effect on the circulating insulin levels in LZR, UCMS increased ($p < .05$) and exercise decreased ($p < .05$) circulating insulin levels in OZR when compared to their respective controls. Although glucose levels were significantly higher in OZR (21.4%, $p < .001$) than in age-matched LZR under the control conditions, the experimental interventions did not significantly affect glucose levels in LZR and OZR.

There was also an increase in the circulating total cholesterol levels among all groups when compared OZR to LZR ($p < .001$). Both exercise ($p < .05$) and UCMS/exercise ($p < .001$) reduced the circulating total cholesterol levels in OZR with no effect in LZR when compared to the controls. The effect of obesity was noted in the amount of the circulating triglyceride levels among all groups when compared OZR to LZR ($p < .001$). However, UCMS, exercise, and UCMS/exercise have no significant impact on the circulating triglyceride levels in LZR and OZR when compared to their respective controls.

A rise in the mean artery pressure (MAP) was noted in the OZR compared with the LZR under control ($p < .01$), UCMS ($p < .01$), and exercise ($p < .05$) conditions. While UCMS ($p < .01$) only increased the MAP in LZR, both UCMS ($p < .01$) and exercise ($p < .05$) significantly raised MAP in OZR. Serum levels of corticosterone were significantly increased in OZR control ($p < .01$), and exercise ($p < .05$) groups compared to LZR. In the LZR group, UCMS ($p < .05$), exercise ($p < .01$), and UCMS/exercise ($p < .05$) resulted in increased corticosterone levels versus LZR control, whereas only UCMS ($p < .05$) and exercise ($p < .05$) increased the serum levels of corticosterone in OZR. Moreover, the coat score (a behavioral measure of stress) of OZR under UCMS ($p < .05$), exercise ($p < .05$), and UCMS/exercise ($p < .05$) conditions were higher compared with LZR under the same experimental conditions, indicating heightened stress levels in OZR groups. The combination of UCMS and exercise consistently resulted in an increase in coat score which suggested poor grooming and heightened stress in LZR ($p < .05$) and OZR ($p < .05$) compared to their respective controls.

3.2 | Visceral adipose tissue cellularity in LZR and OZR

To determine the effects of UCMS and/or exercise on VAT cellularity in LZR and OZR, visceral adipose tissue was stained with H&E (shown in Figure 1A,B). The tissue contained typical white adipocytes, characterized by unilocular lipid droplets. Quantitation of adipocyte cellularity showed an increase in size distribution in the OZR compared with LZR (Figure 1C).

The histomorphometry of VAT showed that OZR had hypertrophic visceral adipocytes of about 40%–60% higher in the analysis that compared OZR to LZR (Figure 1D, $p < .0001$), irrespective of the experimental conditions.

We then evaluated the effects of the experimental interventions on VAT. In LZR, only UCMS/exercise significantly decreased the average adipocyte size and neither exercise nor UCMS induced a change in VAT when compared to the control. We did not observe any change in visceral average adipocyte size in OZR in response to UCMS, exercise, or UCMS/exercise compared to the control group. However, a significant change was noted between OZR UCMS versus OZR exercise with a significant decrease in VAT size in OZR exercise compared to OZR UCMS (Figure 1D, $p < .05$).

We further characterized the distribution of adipocyte size in VAT in response to the various threats in LZR and OZR. We observed a bimodal shape in the distribution of visceral adipocyte sizes in the control groups of LZR (Figure 1E, black bar) and OZR (Figure 1F, black bar), characterized by a fraction of smaller adipocytes and a fraction of large adipocytes, as previously described.[31,32] We classified the area of adipocytes less than 4000 μm^2 as smaller adipocytes and the proportion of adipocytes with the size exceeding 4000 μm^2 as hypertrophied adipocytes.[33,34]

Smaller adipocytes were more prevalent in VAT of LZR than the hypertrophied adipocytes and accounted for 77% of the adipocyte population (Figure 1E). The peak in the small size falls around 2250–2999 μm^2 and the other peak for the larger adipocytes falls at the maximal observed area of >4500 μm^2 (Figure 1E). The proportion of hypertrophic adipocytes present in the maximal observed area of >4500 μm^2 (23%, Figure 1E, black bar) was reduced significantly in response to UCMS (4.25%, $p < .001$), exercise (4.3%, $p < .001$), and UCMS/exercise (0.8%, $p < .001$). This suggests that the experimental interventions increased the population of smaller adipocytes from 77% in the control group to about 90%–98% in the experimental groups.

TABLE 2 Phenotypic characteristics of the LZR and OZR.

	LZR				OZR			
	Con	UCMS	Ex	UCMS/Ex	Con	UCMS	Ex	UCMS/Ex
BW (g)	407.1 ± 14.2	344.4 ± 14.9*	348.0 ± 10.4**	350.1 ± 12.5*	658.3 ± 11.2$^{\&\&\&}$	583.9 ± 13.4***$^{\&\&\&}$	613.4 ± 20.2$^{\&\&\&}$	585.5 ± 6.3***$^{\&\&\&}$
Glu (mg/dL)	139.6 ± 9.4	154.4 ± 13.3	126.4 ± 14	132.9 ± 6.6	215.4 ± 13$^{\&\&\&}$	207.8 ± 40.8	128 ± 0	177.1 ± 19.9
Insulin (ng/mL)	1.2 ± 0.2	2.1 ± 0.4	1.4 ± 0.3	1.8 ± 0.4	6.6 ± 1.1$^{\#\#\#}$	7.8 ± 1.5*$^{\#\#}$	4.6 ± 1*$^{\#\#}$	6.2 ± 1$^{\#\#}$
Cort (ng/mL)	113.7 ± 23.5	257.4 ± 33.1*	200.3 ± 29.7**	318.9 ± 75.9*	166.2 ± 13.3$^{\&\&}$	215.8 ± 13.6*	274.9 ± 36.4*$^{\&}$	168.0 ± 23.1^{+}
TG (mg/dL)	25 ± 3	54 ± 16	31 ± 3	36 ± 3	124 ± 8$^{\#\#\#}$	114 ± 14$^{\#\#\#}$	82 ± 15$^{\#\#\#}$	103 ± 16$^{\#\#\#}$
TC (mg/dL)	86 ± 4	87 ± 5	95 ± 6	88 ± 2	256 ± 26$^{\#\#\#}$	213 ± 17$^{\#\#\#}$	181 ± 8*$^{\#\#\#}$	187 ± 11*$^{\#\#\#}$
Coat scores (AU)	0.3 ± 0.1	0.8 ± 0.2	0.3 ± 0.1	0.9 ± 0.3*	1.1 ± 0.4	2.4 ± 0.6$^{\&}$	1.4 ± 0.4$^{\&}$	2.7 ± 0.6*$^{\&}$
MAP (mmHg)	117.6 ± 1.8	130.5 ± 3.4**	123.1 ± 6.1	118 ± 6.3	129.7 ± 3.1$^{\&\&}$	146.9 ± 3.9**$^{\&\&}$	145.3 ± 4.8*	135.3 ± 4.9

Note: Body weight (BW) was measured in LZR and OZR under control, UCMS, exercise, and UCMS/exercise conditions following 8 weeks of UCMS and/or exercise interventions. Results are presented as the mean of BW ± SEM. LZR control versus OZR control, $p < .001$, $n = 8$; LZR UCMS versus OZR UCMS, $p < .001$, $n = 4–7$; LZR exercise versus OZR exercise, $p < .001$, $n = 6–7$; LZR UCMS/exercise versus OZR UCMS/exercise, $p < .001$, $n = 5–8$. LZR control versus LZR exercise, $p < .001$, $n = 7–8$; LZR control versus LZR UCMS/exercise, $p < .05$, $n = 5–8$; OZR control versus OZR UCMS, $p < .001$, $n = 7–8$; OZR control versus OZR UCMS/exercise, $p < .001$, $n = 8$. Plasma glucose (Glu) was measured in LZR and OZR under control, UCMS, exercise, and UCMS/exercise conditions. Results are presented as the mean of Glu ± SEM. LZR control versus OZR control, $p < .001$, $n = 7–8$. The level of insulin was measured in LZR and OZR under control, UCMS, exercise, and UCMS/exercise conditions. Results are presented as the mean of insulin ± SEM. LZR control versus OZR control, $p < .001$, $n = 8$; LZR UCMS versus OZR UCMS, $p < .01$, $n = 8$; LZR exercise versus OZR exercise, $p < .01$, $n = 8$; LZR UCMS/exercise versus OZR UCMS/exercise, $p < .01$, $n = 8$; OZR control versus OZR UCMS, $p < .05$, $n = 8$; OZR control versus OZR exercise, $p < .05$, $n = 8$. Circulating corticosterone (Cort) level was measured in LZR and OZR under control, UCMS, exercise, and UCMS/exercise conditions. Results are presented as the mean of Cort ± SEM. LZR control versus LZR UCMS, $p < .05$, $n = 8$; LZR control versus LZR exercise, $p < .01$, $n = 8$; LZR control versus LZR UCMS/exercise, $p < .05$, $n = 8$; LZR control versus OZR control, $p < .01$, $n = 8$; LZR exercise versus OZR exercise, $p < .05$, $n = 8$; OZR control versus OZR UCMS, $p < .05$, $n = 8$; OZR control versus OZR exercise, $p < .05$, $n = 8$; OZR exercise versus OZR UCMS/exercise, $p < .05$, $n = 8$. The level of plasma triglycerides (TG) was measured in LZR and OZR under control, UCMS, exercise, and UCMS/exercise conditions. Results are presented as the mean of plasma TG ± SEM. LZR control versus OZR control, $p < .001$, $n = 8$; LZR UCMS versus OZR UCMS, $p < .001$, $n = 8$; LZR exercise versus OZR exercise, $p < .001$, $n = 8$; LZR UCMS/exercise versus OZR UCMS/exercise, $p < .001$, $n = 8$. The level of total cholesterol (TC) was measured in LZR and OZR under control, UCMS, exercise, and UCMS/exercise conditions. Results are presented as the mean of TC ± SEM. LZR control versus OZR control, $p < .001$, $n = 8$; LZR UCMS versus OZR UCMS, $p < .001$, $n = 8$; LZR exercise versus OZR exercise, $p < .001$, $n = 8$; LZR UCMS/exercise versus OZR UCMS/exercise, $p < .001$, $n = 8$; OZR control versus OZR exercise, $p < .05$, $n = 8$; OZR control versus OZR UCMS/exercise, $p < .05$, $n = 8$. Coat score was measured in LZR and OZR under control, UCMS, exercise, and UCMS/exercise conditions. Results are presented as the mean of coat score ± SEM. LZR UCMS versus OZR UCMS, $p < .05$, $n = 8$; LZR exercise versus OZR exercise, $p < .05$, $n = 8$; LZR UCMS/exercise versus OZR UCMS/exercise, $p < .05$, $n = 8$. Mean artery pressure (MAP) was measured in LZR and OZR under control, UCMS, exercise, and UCMS/exercise conditions. Results are presented as the mean of MAP ± SEM. LZR control versus OZR control, $p < .01$, $n = 6–7$; LZR UCMS versus OZR UCMS, $p < .01$, $n = 7–8$; LZR UCMS/exercise versus OZR UCMS/exercise, $p < .001$, $n = 7$; OZR control versus OZR UCMS, $p < .001$, $n = 6–7$. *$p < .05$ versus Control within the same genotype (i.e., LZR or OZR), $^{\&\&\&}p < .001$, $^{\&\&}p < .01$, $^{\&}p < .05$ for LZR versus OZR, $^{+}p < .05$ for exercise versus UCMS/exercise. The statistical differences between LZR and OZR under control, UCMS, exercise, and UCMS/exercise conditions were determined by unpaired *t*-test, and the effects of UCMS and/or exercise were determined by one-way ANOVA followed by a Tukey post hoc test to compare the mean for different groups within the same strain. Data expressed as means ± SD.

Abbreviations: AU, arbitrary unit; BW, body weight; Cort, corticosterone; Glu, glucose; Ins, insulin; LZR, lean Zucker rats; MAP, mean arterial pressure; OZR, obese Zucker rats; TC, total cholesterol; TG, triglycerides.

*$p < .05$ versus control within the same genotype (i.e., LZR or OZR), $^{\#\#\#}p < .001$, $^{\#\#}p < .01$, $^{\#}p < .05$ for LZR versus OZR, LZR versus OZR are also shown by $^{\&}p < .05$, $^{\&\&}p < .01$ and $^{\&\&\&}p < .001$. $^{\sim}p < .05$ for UCMS versus exercise.

In OZR, hypertrophied adipocytes were predominant in VAT and accounted for 69% of the cell population (Figure 1F). Compared to the control, there was no significant change in the population of smaller and hypertrophic adipocytes in VAT of OZR. However, exercise training significantly reduced the proportion of hypertrophic adipocytes (8.3%, Figure 1F) in the fraction of largest adipocytes of >12000 μm^2 category when compared UCMS (21.1%, $p < .05$) and UCMS/exercise (18.1%, $p < .05$).

3.3 | Pericardial adipose tissue cellularity in LZR and OZR

Next, we quantified adipose cellularity in PAT of LZR and OZR and evaluated the effects of the experimental interventions on PAT. In contrast to VAT morphology, PAT contained smaller adipocytes and less proportion of brown-like adipocytes dispersed with PAT in LZR (Figure 2A) and OZR (Figure 2B). The individual data points collected from PAT cellularity measurement showed more concentrated smaller adipocyte sizes in LZR than in OZR (Figure 2C). Unlike VAT cellularity, we did not observe any effect of obesity on PAT cellularity in control, UCMS or UCMS/exercise groups, however, exercised OZR had pericardial adipocyte size of about 56% ($p < .05$) higher than the exercised LZR (Figure 2D). We then evaluated the impacts of the experimental interventions on PAT cellularity. In LZR, there was no notable change in the average adipocytes' size of PAT in both LZR and OZR in response to UCMS and/or exercise (Figure 2D). Next, we analyzed the size distribution of PAT to determine the effects of the experimental interventions. Regardless of the experimental interventions, the distribution of pericardial adipocyte sizes in LZR (Figure 2E) is characterized by positive skewness and a shift towards hyperplastic adipocytes characterized by a 100% proportion of smaller adipocytes (<4000 μm^2). We noted a significant increase in the proportion of smaller adipocytes of about 50% in the category of 450–899 μm^2 in response to UCMS/exercise when compared to control (43.6%, $p < .05$, Figure 2F) or UCMS (44%, $p < .05$, Figure 2F). This corresponds with the decrease in the proportion of adipocytes in the category of 1800–2249 μm^2 when compared UCMS/exercise (1.3%) to the control (3.5%, $p < .05$, Figure 2F) or UCMS (3.1%, $p < .05$, Figure 2F).

PAT from both LZR and OZR displayed characteristics of cellular heterogeneity, composed of both white and brown-like adipocytes compared with VAT. To investigate the heterogeneity of PAT, tissue cellularity was analyzed further by breaking down the surface area analysis into two categories, representing the two types of adipocytes found in PAT. Morphologically, the first type observed resembled white adipocytes, with a larger unilocular lipid droplet and a nucleus pushed to the periphery of the cell. The second type of adipocyte analyzed resembled brown adipocytes, which were smaller, with a densely packed cytosol with multiple lipid droplets (Figure 3A). Further surface area analysis revealed that on average, multilocular adipocytes are approximately 400 μm^2 smaller than unilocular ones (Figure 3B, $p < .0002$). We then investigated the

FIGURE 1 The effects of chronic psychosocial stress and treadmill exercise on the morphology of visceral adipose tissue (VAT). (A) Representative HE section of VAT in LZR (×100 magnification; scale bars: 100 μm). (B) Representative HE section of VAT in OZR (×100 magnification; scale bars: 100 μm). (C) Scatter plot of individual adipocyte size measured directly from the images (D) Average adipocyte size in VAT was measured in LZR and OZR under control, UCMS, exercise, and UCMS/exercise conditions following 8 weeks of UCMS and/or exercise interventions. Results are presented as the mean of adipocyte size ± SEM. LZR control versus OZR control, $p < .001$, $n = 8$; LZR UCMS versus OZR UCMS, $p < .001$, $n = 4–7$; LZR exercise versus OZR exercise, $p < .001$, $n = 6–7$; LZR UCMS/exercise versus OZR UCMS/exercise, $p < .001$, $n = 5–8$; LZR control versus LZR UCMS/exercise, $p < .05$, $n = 5–8$; OZR UCMS versus OZR exercise, $p < .05$, $n = 6–7$. (E) Adipocyte size distribution in LZR showing the adipocyte profile area in different sizing classes. For the adipocyte profile area measuring <750 μm^2, LZR control versus LZR UCMS, $p < .01$, $n = 4–8$. For the adipocyte profile area measuring between 750 and 1499 μm^2, LZR control versus LZR UCMS, $p < .001$ $n = 4–8$; LZR control versus LZR exercise, $p < .001$, $n = 7–8$; LZR control versus LZR UCMS/exercise, $p < .001$, $n = 5–8$; LZR exercise versus LZR UCMS/exercise, $p < .01$, $n = 5–7$. For the adipocyte profile area measuring between 1500 and 2249 μm^2, LZR control versus LZR exercise, $p < .01$, $n = 7–8$; LZR control versus LZR UCMS/exercise, $p < .001$, $n = 5–8$; LZR UCMS versus LZR UCMS/exercise, $p < .01$, $n = 4–5$; LZR exercise versus LZR UCMS/exercise, $p < .05$, $n = 5–7$. For the adipocyte profile area measuring between 2250 and 2999 μm^2, LZR exercise versus LZR UCMS/exercise, $p < .05$, $n = 5–7$. For the adipocyte profile area measuring between 3000 and 3749 μm^2, LZR control versus LZR UCMS/exercise, $p < .01$, $n = 5–8$. For the adipocyte profile area measuring between 3750 and 4499 μm^2, LZR control versus LZR UCMS/exercise, $p < .01$, $n = 5–8$. For the adipocyte profile area measuring >4000 μm^2, LZR control versus LZR UCMS, $p < .001$, $n = 4–8$; LZR control versus LZR exercise, $p < .001$, $n = 7–8$; LZR control versus LZR UCMS/exercise, $p < .001$, $n = 5–8$. (F) Adipocyte size distribution in OZR showing the adipocyte profile area in different sizing classes. For the adipocyte profile area measuring >12000 μm^2, LZR UCMS versus LZR exercise, $p < .01$, $n = 6–7$; LZR exercise versus LZR UCMS/exercise $p < .05$, $n = 6–8$. The statistical differences between LZR and OZR under control, UCMS, exercise, and UCMS/exercise conditions were determined by unpaired *t*-test, and the effects of UCMS and/or exercise were determined by one-way ANOVA followed by a Tukey post hoc test to compare the mean for different groups within the same strain.

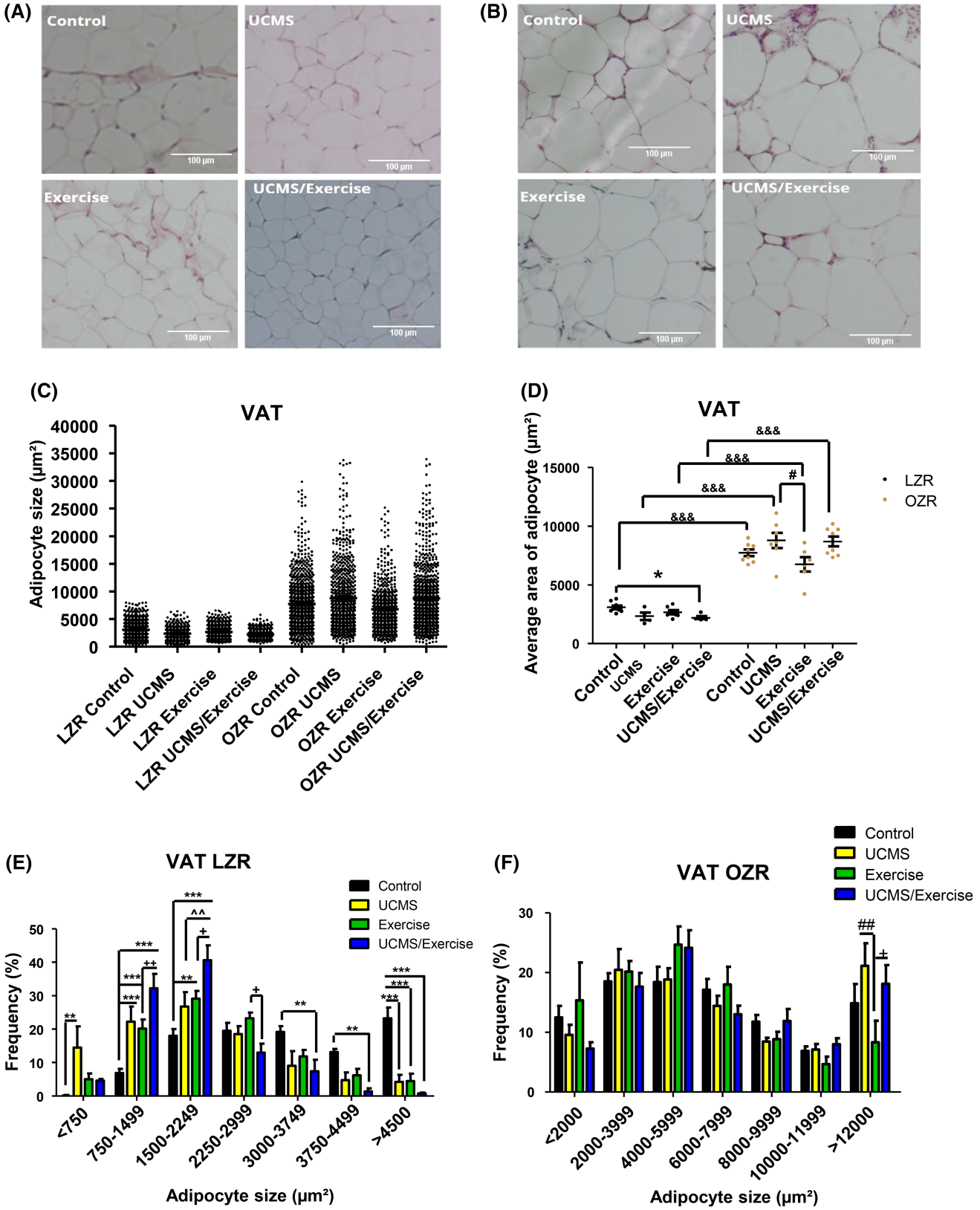

effects of the treatments on the cellularity of both adipocyte populations. In response to UCMS, OZR PAT unilocular adipocytes expanded through hypertrophy, with an approximate increase of 300 μm^2 in surface area relative to the control group (Figure 3C, $p < .037$). We then sought to investigate the relative change in surface area relationship between unilocular and multilocular adipocytes in response to the various treatments, and then compare this ratio obtained for both LZR and OZR (Figure 3D). The effects of UCMS appear to be most

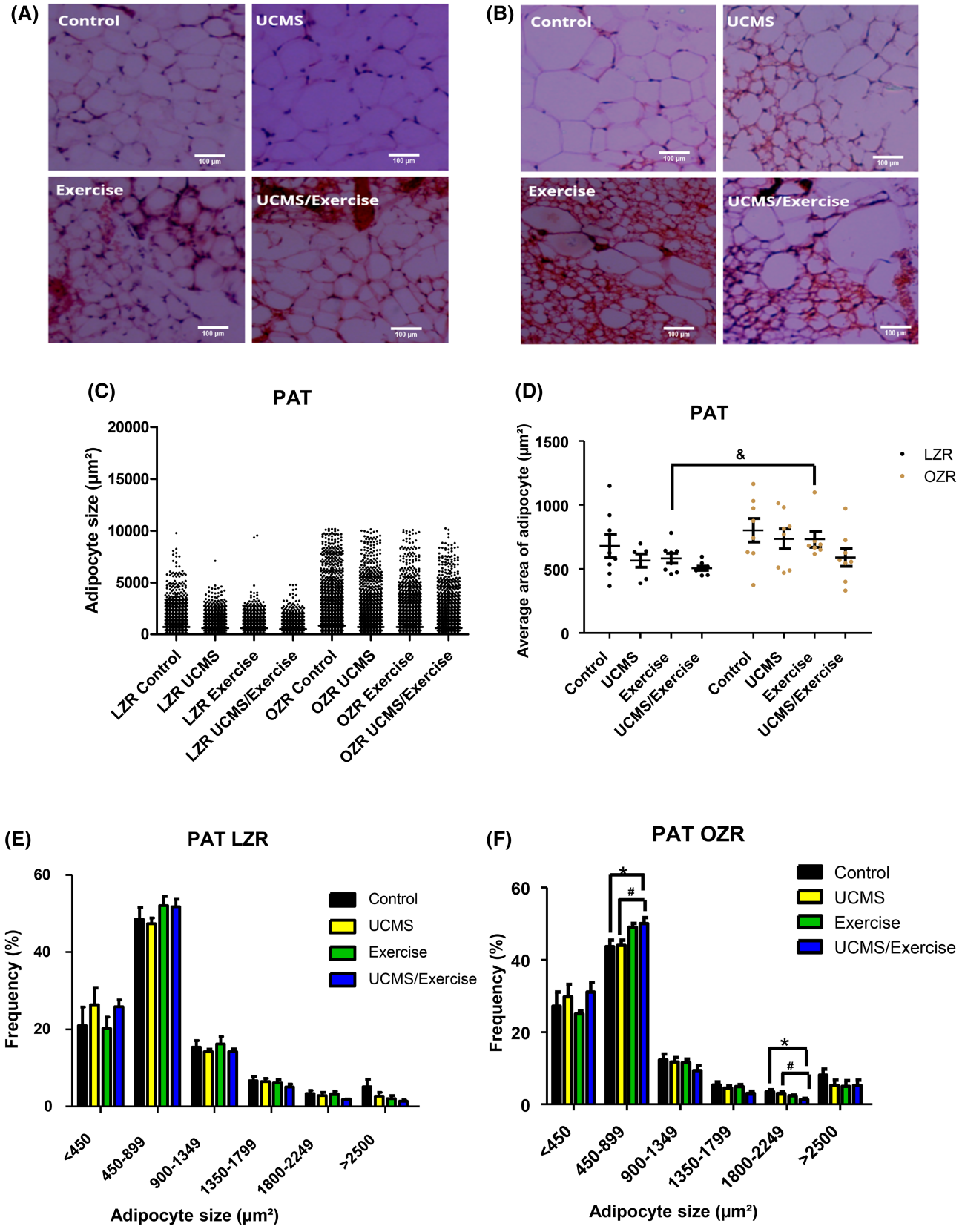

pronounced in OZR than in LZR, where unilocular cells from the obese group were approximately 3 times the size of multilocular adipocytes, whereas this ratio difference was only by 2 in the LZR group (Figure 3D, $p < .01$). The results in Figure 3D indicate that the OZR group were more sensitive to the effects of exercise, as the surface area ratio between the unilocular and multilocular group decreased to approximately 2, which is

FIGURE 2 The effects of chronic psychosocial stress and treadmill exercise on pericardial adipose tissue (PAT) cellularity. (A) Representative HE section of PAT in LZR (×100 magnification; scale bars: 100 μm). (B) Representative HE section of PAT in OZR (×100 magnification; scale bars: 100 μm). (C) Scatter plot of individual adipocyte size measured directly from the images (D) Average adipocyte size in PAT was measured in LZR and OZR under control, UCMS, exercise, and UCMS/exercise conditions following 8 weeks of UCMS and/or exercise interventions. Results are presented as the mean of adipocyte size ± SEM. LZR exercise versus OZR exercise, $p < .05$, $n = 6–8$. (E) Adipocyte size distribution in LZR showing the adipocyte profile area in different sizing classes. (F) Adipocyte size distribution in OZR showing the adipocyte profile area in different sizing classes. For the adipocyte profile area measuring between >450 and 899 μm^2, OZR control versus OZR UCMS/exercise, $p < .05$, $n = 8$; OZR UCMS versus OZR UCMS/exercise $p < .05$, $n = 6–8$. For the adipocyte profile area measuring >1800–2249 μm^2, OZR control versus OZR UCMS/exercise, $p < .05$, $n = 8$; OZR UCMS versus OZR UCMS/exercise $p < .05$, $n = 6–8$. The statistical differences between LZR and OZR under control, UCMS, exercise, and UCMS/exercise conditions were determined by unpaired *t*-test, and the effects of UCMS and/or exercise were determined by one-way ANOVA followed by a Tukey post hoc test to compare the mean for different groups within the same strain.

very similar to the ratio obtained for the LZR group, suggesting that exercise decreased the difference in surface area between unilocular to multilocular adipocytes in the OZR group (Figure 3D, $p < .01$). However, this effect was no longer seen in the OZR group when exercise was combined with UCMS. OZR Unilocular adipocytes returned to being 3 times the size of multilocular adipocytes, suggesting that the presence of psychosocial stress contributes to the increased difference in surface area between white and brown-like adipocytes. We next considered the second mechanism by which adipose tissue remodels; hyperplasia. To do so, we counted the number of each cell type separately and then divided and then expressed the data as a percentage for both unilocular and multilocular adipocytes. The results suggest that OZR PAT underwent an increase in brown-like adipocytes in response to the combination of UCMS and exercise (Figure 3E, $p < .0152$). Figure 3C,D indicate that the surface area of PAT unilocular adipocytes from the OZR group increased, suggesting that in response to stress, PAT from OZR remodels predominantly through hypertrophy, whereas the results shown in Figure 3E suggest that the combination of both UCMS and exercise favors a shift in the number of multilocular adipocytes, which is indicative of remodeling through hyperplasia.

3.4 | Regional and phenotypic selectivity in adipose tissue fibrosis

To determine the role of adipose depot-specific differences in the development of adipose tissue fibrosis in LZR and OZR and the effects of the experimental interventions, we quantified the amount of collagen accumulation in VAT (Figure 4A,B) and PAT (Figure 4C,D) using picrosirius red staining. We observed higher levels of fibrosis in PAT compared with VAT. The 8-week of UCMS protocol decreased fibrosis in PAT of OZR compared to the OZR control (Figure 4E, $p < .05$). Considering the size differences and mechanism of adipose tissue expansion between VAT and PAT, particularly in OZR, we evaluated the differences in fibrosis between the VAT and PAT under each experimental condition. PAT obtained from OZR showed higher levels of fibrosis when compared to VAT in the control (Figure 4F, $p < .05$) and UCMS/exercise (Figure 4F, $p < .05$) groups.

3.5 | The effects of chronic psychosocial stress and treadmill exercise on markers of lipogenic, thermogenic, and adipogenic mRNA expression in adipose tissue obtained from LZR and OZR

To assess the effects of UCMS and/or exercise on the lipogenic, thermogenic, and adipogenic responses of VAT and PAT, LZR, and OZR were exposed to environmental stressors and treadmill exercise for 8 weeks and compared to their respective controls. There was no significant change in VAT in the analysis that compared OZR to LZR irrespective of their experimental conditions; however, UCMS/exercise significantly downregulated the expression of leptin mRNA in PAT of OZR when compared with LZR (Figure 5A, $p < .01$). We then determined the effects of UCMS and/or exercise on leptin mRNA expression. We observed an upregulation of leptin mRNA expression in LZR UCMS/exercise versus LZR exercise (Figure 5A, $p < .01$). UCMS significantly downregulated the expression of leptin mRNA in OZR (Figure 5A, $p < .05$) when compared to control but the expression was unaffected by exercise and UCMS/exercise interventions. We did not observe any change in adipoQ mRNA expression in LZR and OZR in response to the experimental interventions when compared to their respective controls (data not shown). The expression of adipoQ mRNA in PAT was upregulated in OZR UCMS/exercise versus OZR exercise (Figure 5B, $p < .05$).

The gene expression levels of UCP1 were upregulated in VAT in the analysis that compared OZR to LZR in controls (Figure 5C, $p < .05$), UCMS (Figure 5C, $p < .01$), and

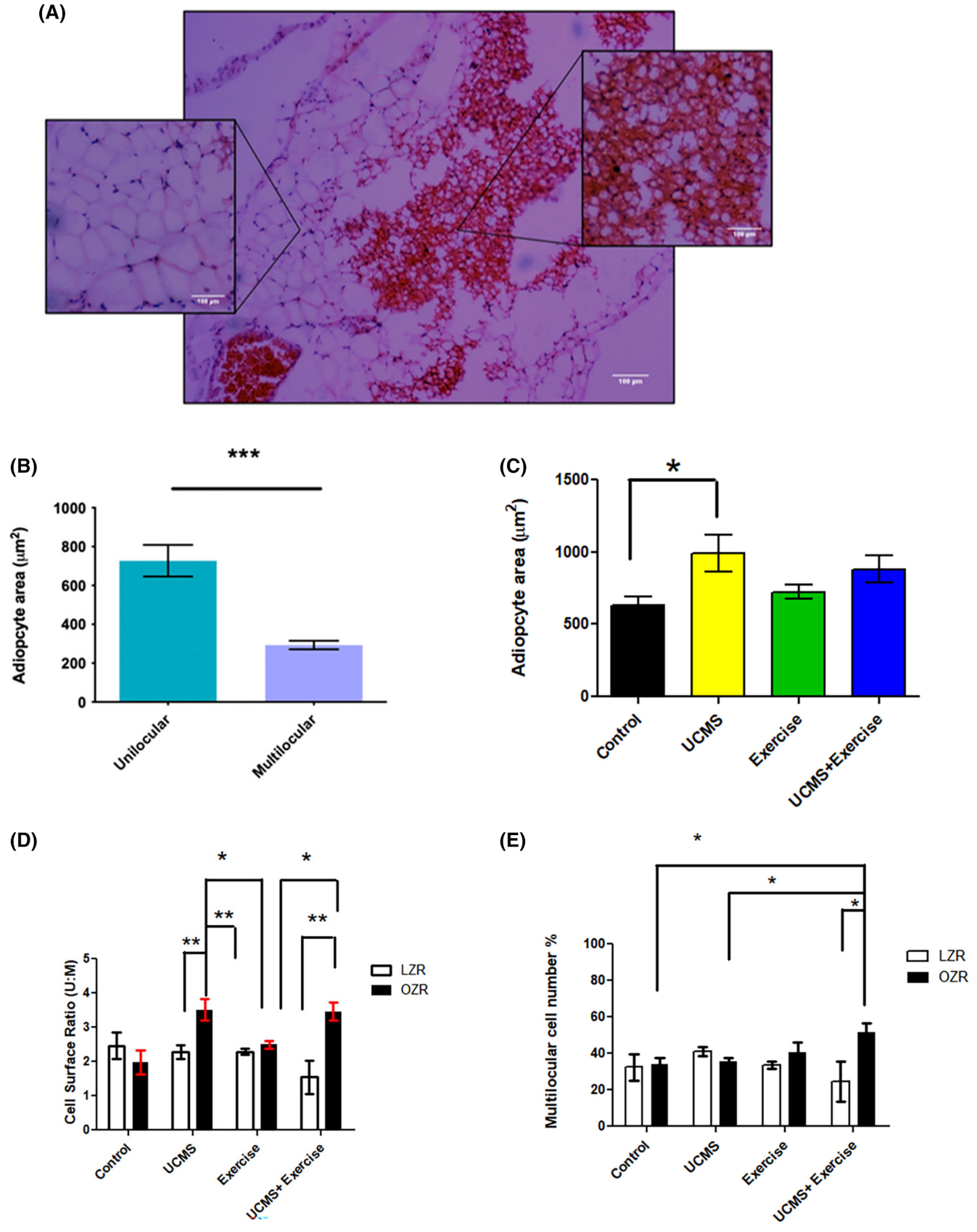

UCMS/exercise (Figure 5C, $p < .05$). Considering that the morphological analysis showed that PAT was a beige depot, we compared the expression of UCP1 mRNA in PAT to VAT. The expression of UCP1 mRNA was upregulated in PAT when compared to VAT in LZR (Figure 5D, $p < .05$).

FIGURE 3 Pericardial adipose tissue shows evidence of cellular heterogeneity, composed of both unilocular and multilocular adipocytes both of which remodel differently in response to UCMS and the combination of exercise and UCMS. (A) Lean control H&E-stained PAT section containing two types of fat cells. The magnifying box on the left displays white-like adipocytes with a single large lipid droplet occupying most of the cell. The second cell type is a brown-like adipocyte, with multiple small lipid droplets occupying the cytosol (×100 magnification, scale bars 100 μm). (B) Multilocular adipocytes have a smaller surface area when compared to unilocular adipocytes. (C) UCMS causes hypertrophy in PAT unilocular adipocytes from obese Zucker rats. (D) Cell surface ratio unilocular: multilocular comparison between LZR and OZR models. OZR adipocytes were more sensitive to UCMS as the unilocular cells were three times the size of the multilocular adipocytes, this difference is significantly larger than that observed in the lean condition. When comparing this ratio in the OZR group between the UCMS and the exercise group, exercise alone reduced the difference in surface area between unilocular and multilocular adipocytes. The combination of UCMS and exercise increased the surface area difference between the two cell types in the OZR group compared to the cells counted from the LZR group. (E) Comparison of the cell number percentage of multilocular adipocytes in lean and obese samples. In response to the combination of UCMS and exercise, there appears to be an increase in multilocular adipocytes in obese PAT. Data presented as Mean ± SEM, all groups $n = 6$, Comparisons in Figure 4C were done using a one-way ANOVA followed by Tukey post hoc test to compare the means within the same strain. LZR Unilocular versus Multilocular ***$p < .0002$. OZR Unilocular surface area control versus UCMS *$p < .037$. Multilocular cell number % UCMS + exercise OZR versus LZR *$p < .0449$. Multilocular cell number % OZR UCMS + exercise versus Control *$p < .0152$. Pairwise comparisons were calculated using a Student t-test, all levels of significance were at $p < .05$. UCMS OZR versus LZR **$p < .0081$, OZR UCMS versus exercise *$p < .0127$. OZR exercise versus UCMS + exercise **$p < .0069$. UCMS + exercise LZR versus OZR **$p < .0067$.

When we compared OZR to LZR under the same experimental conditions, UCMS significantly upregulated the expression of PPAR-γ in VAT (Figure 5E, $p < .05$) but downregulated PPAR-γ mRNA expression in PAT (Figure 5E, $p < .05$). There was no notable change in the expression of PPAR-γ mRNA in VAT across the experimental interventions when compared to control in both LZR and OZR. However, UCMS (Figure 5F, $p < .05$) and exercise (Figure 5F, $p < .05$) significantly downregulated the expression of PPAR-γ mRNA in PAT of OZR when compared to control. Additionally, FABP4 and PGC1a were also measured at the level of the message but showed no change in expression levels.

3.6 | The effects of chronic psychosocial stress and treadmill exercise on the key molecules involved in insulin signaling in adipose tissue obtained from LZR and OZR

We then determined the transcriptional profiles of the key molecules involved in insulin signaling. The evaluation of the expression of IRS1 in OZR compared to LZR showed that exercise upregulated IRS1 mRNA in VAT (Figure 6A, $p < .01$) of OZR exercise versus LZR exercise. In contrast, exercise downregulated IRS1 mRNA in PAT (Figure 6B, $p < .01$) of OZR exercise versus LZR exercise. In response to the experimental intervention, exercise training downregulated IRS1 mRNA expression (Figure 6A, $p < .01$) in VAT of LZR and upregulated IRS1 mRNA expression (Figure 6A, $p < .01$) in VAT of OZR when compared to their respective controls. Furthermore, we observed downregulation of IRS1 mRNA expression in VAT of LZR exercise compared to LZR UCMS (Figure 6A, $p < .05$). In PAT, exercise training upregulated IRS1 mRNA expression (Figure 6B, $p < .05$) in LZR and downregulated IRS1 mRNA expression (Figure 6B, $p < .05$) in OZR when compared to their controls. We also noted a downregulation of IRS1 mRNA expression in PAT of LZR UCMS/exercise compared to LZR exercise (Figure 6B, $p < .05$).

We showed that exercise (Figure 6C, $p < .05$) and UCMS/exercise (Figure 6C, $p < .05$) in OZR upregulated HSD11B1 mRNA in VAT when compared to LZR under the same experimental conditions. Exercise, on the other hand, downregulated HSD11B1 mRNA in PAT (Figure 6D, $p < .05$) when comparing the OZR group to LZR group. However, there was no notable change in the expression of HSD11B1 mRNA in VAT (Figure 6C) and PAT (Figure 6D) across the experimental interventions when compared to controls.

In addition, we demonstrated that exercise (Figure 6E, $p < .05$) and UCMS/exercise (Figure 6E, $p < .05$) upregulated the expression of calnexin mRNA in VAT and both exercise (Figure 6F, $p < .01$) and UCMS/exercise (Figure 6F, $p < .01$) suppressed calnexin mRNA in PAT in the analysis that compared OZR to LZR. However, there was no notable change in the expression of calnexin mRNA in VAT (Figure 6E) and PAT (Figure 6F) across the experimental interventions when compared to controls.

3.7 | The effects of chronic psychosocial stress and treadmill exercise on inflammatory and fibrotic markers of adipose tissue obtained from LZR and OZR

To investigate whether VAT and PAT had altered the transcriptional profile of inflammatory markers in response to obesity and experimental interventions, we assessed the expression of inflammatory markers in VAT

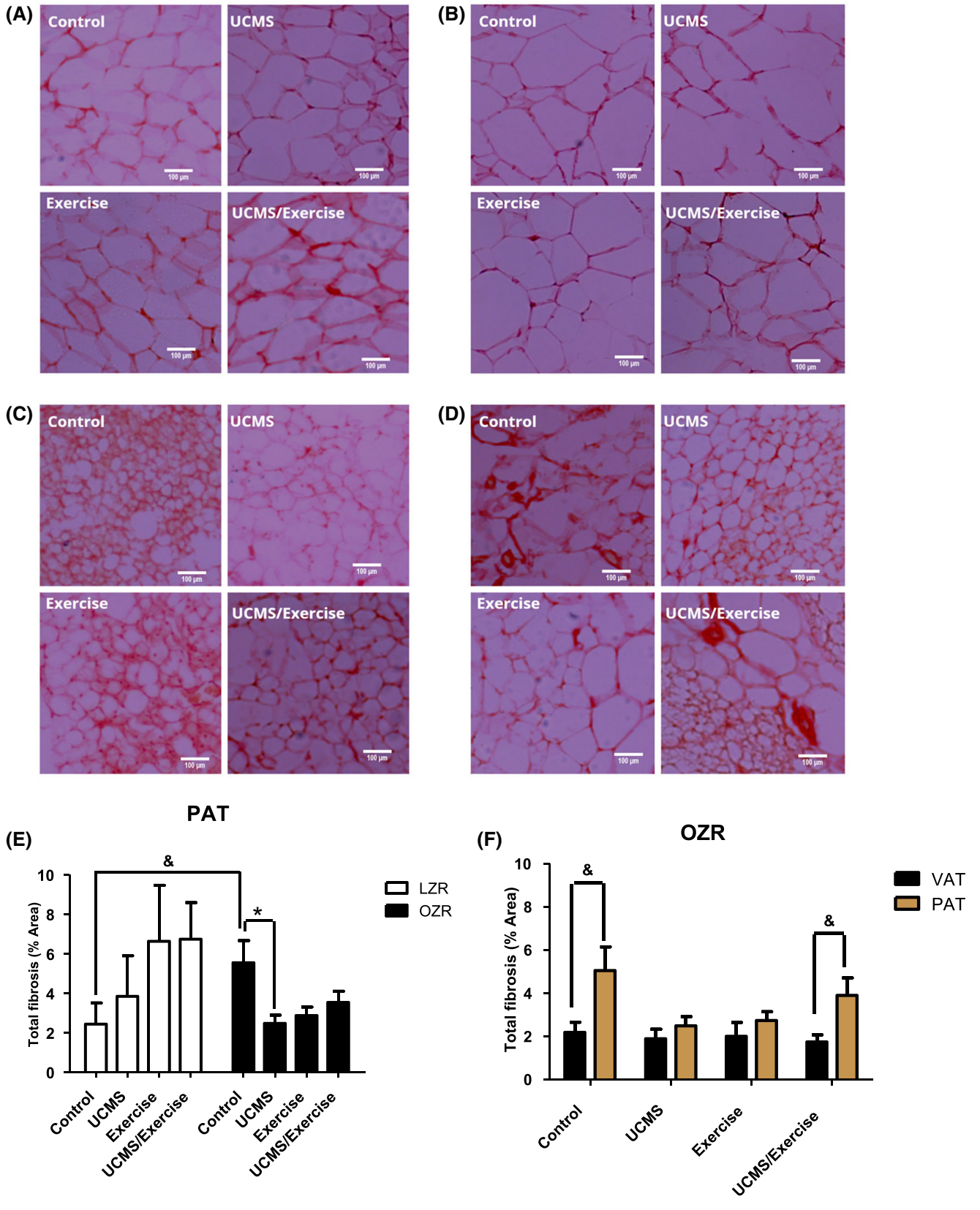

and PAT of LZR and OZR. The evaluation of the expression of TNF-α in the analysis that compared OZR to LZR showed that UCMS/exercise downregulated TNF-α mRNA (Figure 7A, $p < .05$) in VAT irrespective of the experimental conditions. The expression of TNF-α was downregulated in PAT when comparing OZR UCMS versus LZR UCMS (Figure 7B, $p < .01$). There was no notable change in the expression of TNF-α mRNA in VAT in both

FIGURE 4 Increased fibrosis in obese pericardial adipose tissue was reduced by UCMS. (A) Representative PSR-section of VAT in LZR (×100 magnification; scale bars: 100 μm). (B) Representative PSR-section of VAT in OZR (×100 magnification; scale bars: 100 μm). (C) Representative PSR-section of PAT in LZR (×100 magnification; scale bars: 100 μm). (D) Representative PSR-section of VAT in OZR (×100 magnification; scale bars: 100 μm). (E) Total fibrosis in PAT is expressed as a percentage of the total cellular membranes in LZR and OZR under control, UCMS, exercise, or UCMS/exercise conditions. Results are presented as the mean of percentage total fibrosis ± SEM. LZR control versus OZR control, $p < .05$, $n = 6–7$; OZR control versus OZR UCMS, $p < .05$, $n = 6–8$. (F) Total fibrosis in VAT and PAT are expressed as the percentage of the total cellular membranes in OZR under control, UCMS, exercise, or UCMS/exercise conditions. Results are presented as the mean of percentage total fibrosis ± SEM. VAT control versus PAT control, $p < .05$, $n = 6–7$; VAT UCMS/exercise versus PAT UCMS/exercise, $p < .05$, $n = 7–8$. The statistical differences between LZR and OZR under control, UCMS, exercise, and UCMS/exercise conditions were determined by unpaired *t*-test, and the effects of UCMS and/or exercise were determined by one-way ANOVA followed by a Tukey post hoc test to compare the mean for different groups within the same strain.

LZR and OZR when compared to their respective controls (Figure 7A). In LZR, the expression of TNF-α mRNA in PAT was downregulated by UCMS (Figure 7B, $p < .05$), and UCMS/exercise (Figure 7B, $p < .05$) when compared to control. To help explain the changes in tissue fibrosis observed in the PAT, we also examined the expression of key fibrotic markers periostin (POSTN), connective tissue growth factor (CTGF), tissue metalloproteinase 1&3 (TIMP1 and TIMP3). In OZR, UCMS, exercise, and UCMS/exercise, all resulted in a decreased expression of POSTN, CTGF, and TIMP1 (Figure 7C–E respectively). TIMP3 was only decreased following UCMS treatment (Figure 7F). In LZR, these treatments had no significant impact on these fibrotic markers in PAT. In VAT however, UCMS decreased CTGF expression in LZR relative to controls (Figure S1G) but showed no changes to POSTN (Figure S1F). In VAT, exercise decreased TIMP3 expression and in the OZR the combination of exercise and stress increased TIMP3 expression relative to UCMS only (Figure S1H).

Next, we evaluated the expression of caveolin-1 mRNA in VAT. The analysis that compared OZR to LZR showed that both UCMS (Figure S1D, $p < .05$) and exercise (Figure S1D, $p < .05$) upregulated caveolin-1 mRNA in VAT. In response to the experimental interventions, UCMS significantly elevated the expression of caveolin-1 in OZR VAT (Figure S1D, $p < .05$). Next, we showed that the expression of EMR1 mRNA was suppressed in PAT when comparing OZR exercise to LZR exercise (Figure S1E, $p < .05$).

3.8 | Leptin signaling is necessary for adipocyte hypertrophy but not lipid droplet size

The in vivo data so far indicate that remodeling of adipose tissue in response to stress and exercise is different between LZR and OZRs. However, since the OZRs have deficient leptin signaling and obesity, it is unclear which is the most important for mediating the observed effects. To separate the obesogenic effects from downstream leptin signaling, cultured 3T3-L1-derived adipocytes were treated with palmitate (an obesogenic stimulus) and/or Hex to inhibit Jak2 autophosphorylation downstream of the leptin receptor. These experiments were designed to determine the impact of impaired leptin signaling on adipocyte remodeling in response to an obesogenic stimulus. Following these treatments, adipocyte cell size, droplet size, and number measured and shown in Figure 8A–D. To investigate the potency of Hex inhibitor in inhibiting the Jak2 autophosphorylation downstream of the leptin receptor, 3T3-L1 adipocytes were treated with 5 μM Hex for 48 h. Western blotting of 3T3-L1 adipocyte lysates following 48 h of Hex treatment revealed the attenuation of Jak2 autophosphorylation by JAK2 inhibitor. (Figure 8E). The treatment of 3T3-L1 adipocytes with 5 μM Hex for 48 h did not change the adipocyte size, however, while palmitate increased the adipocyte area (Figure 8F, $p < .001$), the combination of Hex and palmitate significantly reduced the adipocyte area (Figure 8F, $p < .001$). To mimic the mechanism of adipocyte expansion when leptin signaling is impaired, the cells were treated with Hex and/or palmitate, and the size of the lipid droplets was measured. The results showed that both palmitate and Hex+palmitate treatments induced significantly cellular hypertrophy (Figure 8G, $p < .001$ respectively) that was inhibited by Hex treatment after 48 h (Figure 8G, $p < .05$). In the palmitate-only group, cellular hypertrophy and increased lipid droplet size was associated with a reduction in droplet number (Figure 8H, $p < .001$) which was further reduced by the addition of Hex. (Figure 8H, $p < .001$). This suggests that the combination of an obesogenic stimulus and inhibition of leptin signaling results in adipocyte whitening.

4 | DISCUSSION

With the increased prevalence of obesity, there is a need to understand how different adipose depots adapt to obesity and physiological stimuli such as exercise and psychosocial

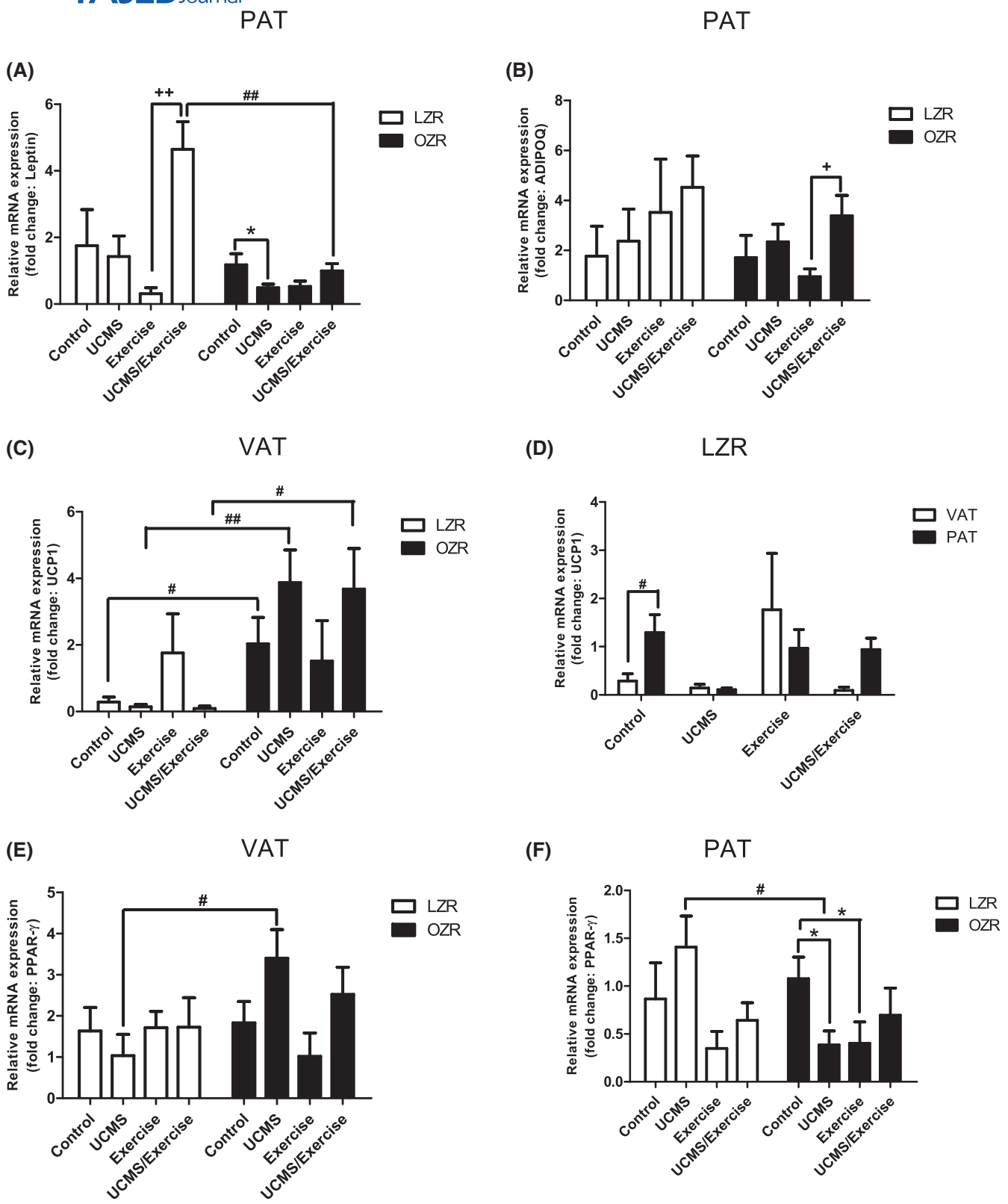

stress. Here we show for the first time that visceral and pericardial adipose tissue display differential remodeling in response to exercise and psychosocial stress and these effects are highly dependent on leptin receptor signaling. Our data indicate that in the presence of leptin receptor signaling, visceral adipose tissue is very plastic and remodels significantly in response to both exercise and psychosocial stress. In contrast, pericardial adipose tissue remodels very little in response to these physiological stimuli. However, the absence of leptin receptor signaling results in pathological remodeling to psychosocial stress that could have significant implications for cardiac physiology.

FIGURE 5 The effects of chronic psychosocial stress and treadmill exercise on lipogenic, thermogenic, and adipogenic mRNA expression in visceral adipose tissue (VAT) and pericardial adipose tissue (PAT) in LZR and OZR. (A) mRNA expression of leptin was measured in PAT obtained from LZR and OZR under control, UCMS, exercise, and UCMS/exercise conditions. Results are presented as fold change in gene expression ± SEM. LZR UCMS/exercise versus OZR exercise, $p < .01$, $n = 6–8$; LZR exercise versus LZR UCMS/exercise, $p < .01$, $n = 4–8$; OZR control versus OZR UCMS, $p < .05$, $n = 5–9$. (B) mRNA expression of adipoQ was measured in PAT obtained from LZR and OZR under control, UCMS, exercise, and UCMS/exercise conditions. Results are presented as fold change in gene expression ± SEM. OZR exercise versus OZR UCMS/exercise, $p < .05$, $n = 6–9$. (C) mRNA expression of UCP1 was measured in VAT obtained from LZR and OZR under control, UCMS, exercise, and UCMS/exercise conditions. Results are presented as fold change in gene expression ± SEM. LZR control versus OZR control, $p < .05$, $n = 7–8$; LZR UCMS versus OZR UCMS, $p < .01$, $n = 5–7$; LZR UCMS/exercise versus OZR UCMS/exercise, $p < .05$, $n = 4–11$. (D) mRNA expression of UCP1 was measured in VAT and PAT obtained from LZR under control, UCMS, exercise, and UCMS/exercise conditions. Results are presented as fold change in gene expression ± SEM. VAT control versus PAT control, $p < .05$, $n = 4–7$. (E) mRNA expression of PPAR-γ was measured in VAT obtained from LZR and OZR under control, UCMS, exercise, and UCMS/exercise conditions. Results are presented as fold change in gene expression ± SEM. LZR UCMS versus OZR UCMS $p < .05$, $n = 6–13$. (F) mRNA expression of PPAR-γ was measured in PAT obtained from LZR and OZR under control, UCMS, exercise, and UCMS/exercise conditions. Results are presented as fold change in gene expression ± SEM. LZR UCMS versus OZR UCMS $p < .05$, $n = 4–9$; OZR control versus OZR UCMS, $p < .05$, $n = 5–9$; OZR control versus OZR versus OZR exercise, $p < .05$, $n = 5–9$. The statistical differences between LZR and OZR under control, UCMS, exercise, and UCMS/exercise conditions were determined by unpaired *t*-test, and the effects of UCMS and/or exercise were determined by one-way ANOVA followed by a Tukey post hoc test to compare the mean for different groups within the same strain.

4.1 | Adipocyte remodeling following stress and exercise in VAT

Zucker rats have been shown to be a good model of human obesity as they display adipose tissue expansion and increased body weight from 2–4 months.[35–38] This increase in body weight is associated with significant VAT adipocyte hypertrophy. Partitioned analysis of the cellularity data demonstrated that in lean animals with normal leptin receptor signaling, both exercise and stress significantly increased the number of smaller adipocytes compared with untreated controls. Combining exercise and stress augmented this reduction in adipocyte size. Interestingly, these changes were not observed in the OZRs with impaired leptin receptor signaling. This suggests that adipocyte remodeling in response to these physiological stimuli requires functional leptin receptor signaling. Additional in vitro experiments using 3T3-derived adipocytes showed that adipocyte remodeling in response to palmitate, that mimics the obesogenic diet, is blocked by Hex treatment which inhibits downstream signaling via the leptin receptor. Interestingly, lipid droplet hypertrophy on the other hand was unaffected by leptin inhibition suggesting that other pathways may regular droplet dynamics within the adipocyte. Leptin signaling has been shown to induce adipose tissue browning,[39] so the whitening induced by palmitate and Hex treatment is in keeping with that finding. It has been previously shown that early exposure of mice to chronic stress disrupts leptin signaling and results in higher vulnerability to becoming obese in adulthood when fed with a moderate Western-style diet.[40] Another study showed that chronic psychosocial stress contributed to the development of obesity, with the selective accumulation of visceral fat in humans.[41] Mechanistically, psychosocial stress is associated with increased plasma corticosterone levels in rodents and cortisol in humans.[42,43] Weight loss is a predominant response to chronic stress in animal studies as previously demonstrated in obesity-prone as well as in obesity-resistant mice,[44] male and female rats[45] and male Wistar rats.[46] However, evidence for weight loss caused by psychosocial stress in humans is limited and contrasts with animal studies. A few studies suggest that weight loss is prominent in lean humans due to an inhibition of food intake by the hyperactivity of the hypothalamic–pituitary–adrenal (HPA) axis under stressful events.[47] While obese subjects gain more weight due to binge eating in response to psychosocial stress.[48–50] Hyperphagia in response to stress has been associated with hyperleptinemia among overweight women.[51,52] A study showed that early exposure of mice to chronic stress disrupts leptin signaling and results in higher vulnerability to developing obesity in adulthood when fed with a moderate Western-style diet.[40] However, our data strongly suggest that the response to psychosocial stress can also be influenced by leptin signaling.

Exercise training offers beneficial effects on healthy individuals, patients with type 2 diabetes mellitus, hypertension, and cardiovascular disease, irrespective of their body weight.[53] In obese individuals, exercise improved physical fitness, increased insulin sensitivity, and lowered plasma lipids and lipoproteins.[54–56] In this study, exercise training significantly reduced weight, reduced blood lipids, and improved glucose homeostasis in the prediabetic OZR, following the 8-week experimental interventions. While exercise training reduced the body weight of LZR, the plasma metabolites remained unchanged since these were already in the normal range. A previous study revealed that obese and prediabetic individuals exhibited weight

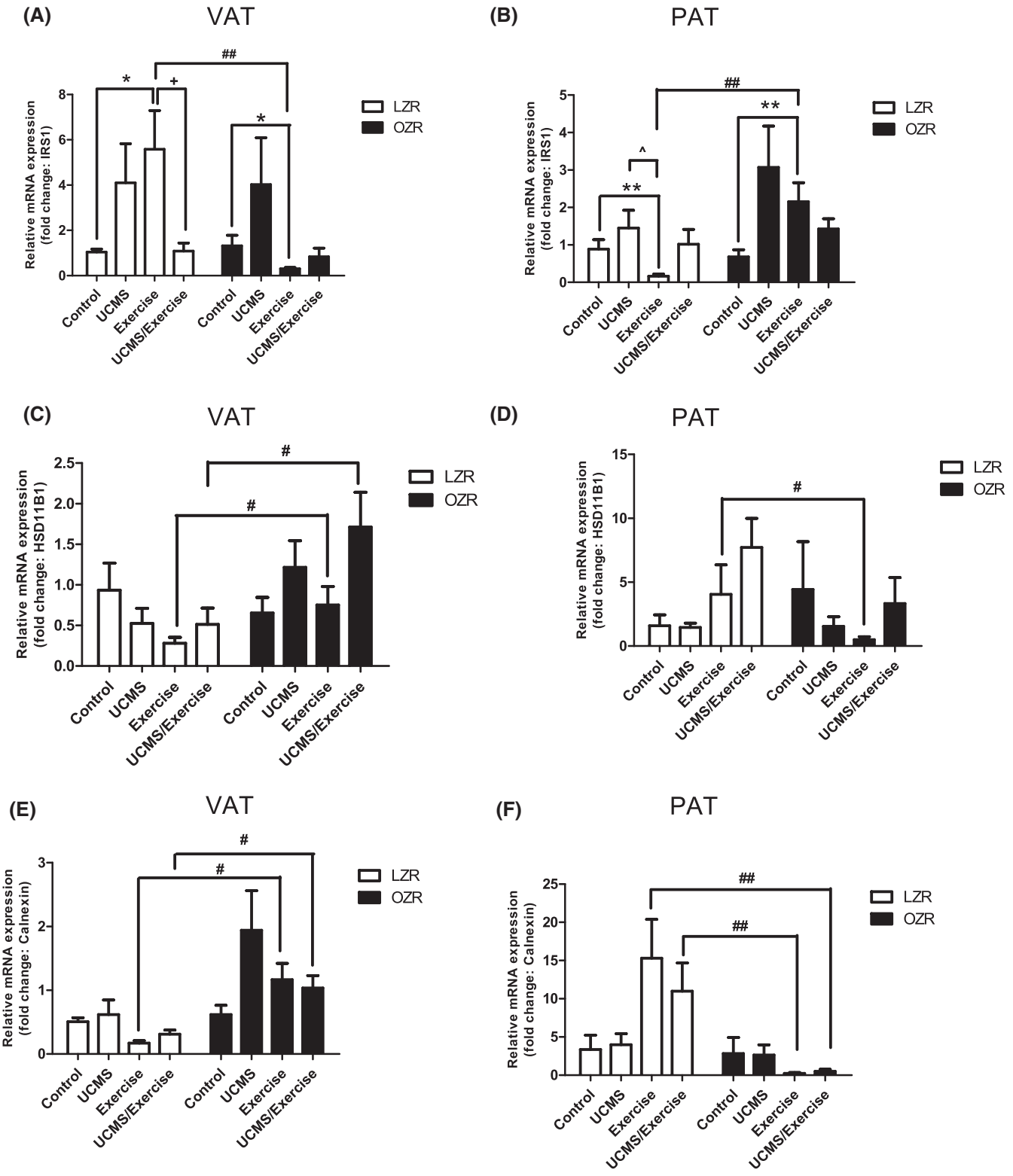

loss and improved metabolic adaptations to exercise training than the normoglycemic older men and women.[57] The differences observed between LZR and OZR could be attributed to the higher energy expenditure in obesity due to their large body size as observed in obese individuals compared with normal-weight individuals.[58] It has been reported that the physiological adaptation to exercise and psychosocial stress share the similarities of hyperactivity of the HPA.[26,59] In our study, both LZR and OZR were subjected to exercise training first and followed by the UCMS stress protocol but is likely to have stressed the animals further.

Exercise training has been known to cause physiological adaptations to white adipose tissue through the

FIGURE 6 The effects of chronic psychosocial stress and treadmill exercise on key molecules for insulin and metabolic signaling in visceral adipose tissue (VAT) and pericardial adipose tissue (PAT) in LZR and OZR. (A) mRNA expression of IRS1 was measured in VAT obtained from LZR and OZR under control, UCMS, exercise, and UCMS/exercise conditions. Results are presented as fold change in gene expression ± SEM. LZR exercise versus OZR exercise, $p < .01$, $n = 4–7$; LZR control versus LZR exercise, $p < .01$, $n = 7–12$; LZR UCMS versus LZR exercise, $p < .05$, $n = 6–7$; OZR control versus OZR exercise, $p < .01$, $n = 4–6$. (B) mRNA expression of IRS1 was measured in PAT obtained from LZR and OZR under control, UCMS, exercise, and UCMS/exercise conditions. Results are presented as fold change in gene expression ± SEM. LZR exercise versus OZR exercise, $p < .01$, $n = 5–7$; LZR control versus LZR exercise, $p < .05$, $n = 5$; LZR exercise versus LZR UCMS/exercise, $p < .05$, $n = 5–11$; OZR control versus OZR exercise, $p < .05$, $n = 5–7$. (C) mRNA expression of HSD11B1 was measured in VAT obtained from LZR and OZR under control, UCMS, exercise, and UCMS/exercise conditions. Results are presented as fold change in gene expression ± SEM. LZR exercise versus OZR exercise, $p < .05$, $n = 6–7$; LZR UCMS/exercise versus OZR UCMS/exercise, $p < .05$, $n = 7–12$. (D) mRNA expression of HSD11B1 was measured in PAT obtained from LZR and OZR under control, UCMS, exercise, and UCMS/exercise conditions. Results are presented as fold change in gene expression ± SEM. LZR exercise versus OZR exercise, $p < .05$, $n = 5–7$. (E) mRNA expression of calnexin was measured in VAT obtained from LZR and OZR under control, UCMS, exercise, and UCMS/exercise conditions. Results are presented as fold change in gene expression ± SEM. LZR exercise versus OZR exercise, $p < .05$, $n = 5–7$; LZR UCMS/exercise versus OZR UCMS/exercise $p < .05$, $n = 7–13$. (F) mRNA expression of calnexin was measured in PAT obtained from LZR and OZR under control, UCMS, exercise, and UCMS/exercise conditions. Results are presented as fold change in gene expression ± SEM. LZR exercise versus OZR exercise, $p < .01$, $n = 5–7$; LZR UCMS/exercise versus OZR UCMS/exercise $p < .01$, $n = 5–11$. The statistical differences between LZR and OZR under control, UCMS, exercise, and UCMS/exercise conditions were determined by unpaired *t*-test, and the effects of UCMS and/or exercise were determined by one-way ANOVA followed by a Tukey post hoc test to compare the mean for different groups within the same strain.

decrease in adipocyte size and lipid content, as well as the browning of white adipose tissue with an increase in mitochondrial proteins.[60] Evidence highlights that moderate exercise induces mobilization of free fatty acids during exercise[61] and attenuates postprandial lipemia[62] and triglycerides.[63,64] Exercise usually induces lipolysis resulting in smaller adipocytes in white adipose tissue such as VAT. Our data clearly demonstrates this in the lean animals but was significantly attenuated in the absence of leptin receptor signaling in the OZR. In these obese animals, only the largest VAT adipocytes showed a significant reduction in size, suggesting resistance to lipolysis in the absence of leptin signaling.

Our study shows that in VAT, adipose tissue remodeling in response to physiological stimuli was associated with significant differences in gene expression which was also influenced by the presence of leptin signaling. Exercise decreased insulin sensitivity as determined by the expression of IRS1 in the presence of leptin receptor signaling, while improving it in its absence. Our data would suggest that this increased insulin sensitivity following exercise could be inhibited by leptin receptor signaling.

Interestingly, the increase in insulin sensitivity following exercise was associated with an increase in caveolin-1 expression. Mechanistically, caveolin has been shown to regulate insulin sensitivity through the PI3K/Akt pathway in VAT and caveolin-1 knockout mice develop significant insulin resistance.[65] Although we did not see any major effects of stress on insulin signaling in VAT, previous work has shown that chronic stress impairs insulin signaling and glucose uptake in VAT in response to insulin stimulation in Fisher rats; but upregulates the intracellular signaling molecules that respond to inflammatory signals through p65 and p38 and subsequently inhibit the phosphorylation of IRS-1.[66] Our data suggest that psychosocial stress was also associated with increased adipogenesis in the absence of leptin signaling suggesting a role in pre-adipocyte expansion. This may explain the stress-dependent increase in the adipogenesis marker PPAR-γ in the OZRs relative to the lean controls.

4.2 | Adipocyte remodeling following stress and exercise in PAT

Very little is known about the remodeling of PAT in response to physiological stimuli, particularly in obesity. Like VAT, PAT has been strongly associated with the prevalence of cardiovascular disease in human adults.[67,68] Although the volume of PAT pad is smaller compared to VAT, it is likely exerting direct paracrine effects on the heart due to its anatomic proximity to the coronary arteries and cardiac muscle via the pericardial fluid.[6] Our study shows for the first time that in obesity, PAT does not expand significantly in obesity unless it is combined with psychosocial stress. We have also shown for the first time that unilocular and multilocular adipocytes respond independently to exercise and psychosocial stress. Moreover, we show for the first time that in the absence of leptin receptor signaling, psychosocial stress results in hypertrophy of the unilocular adipocytes within the PAT depot. This suggests that although the brown-like PAT is generally resistant to hypertrophic expansion, the combination of impaired leptin signaling, and psychosocial stress leads to a pathological phenotype with potentially negative implications for cardiac function. Unlike the

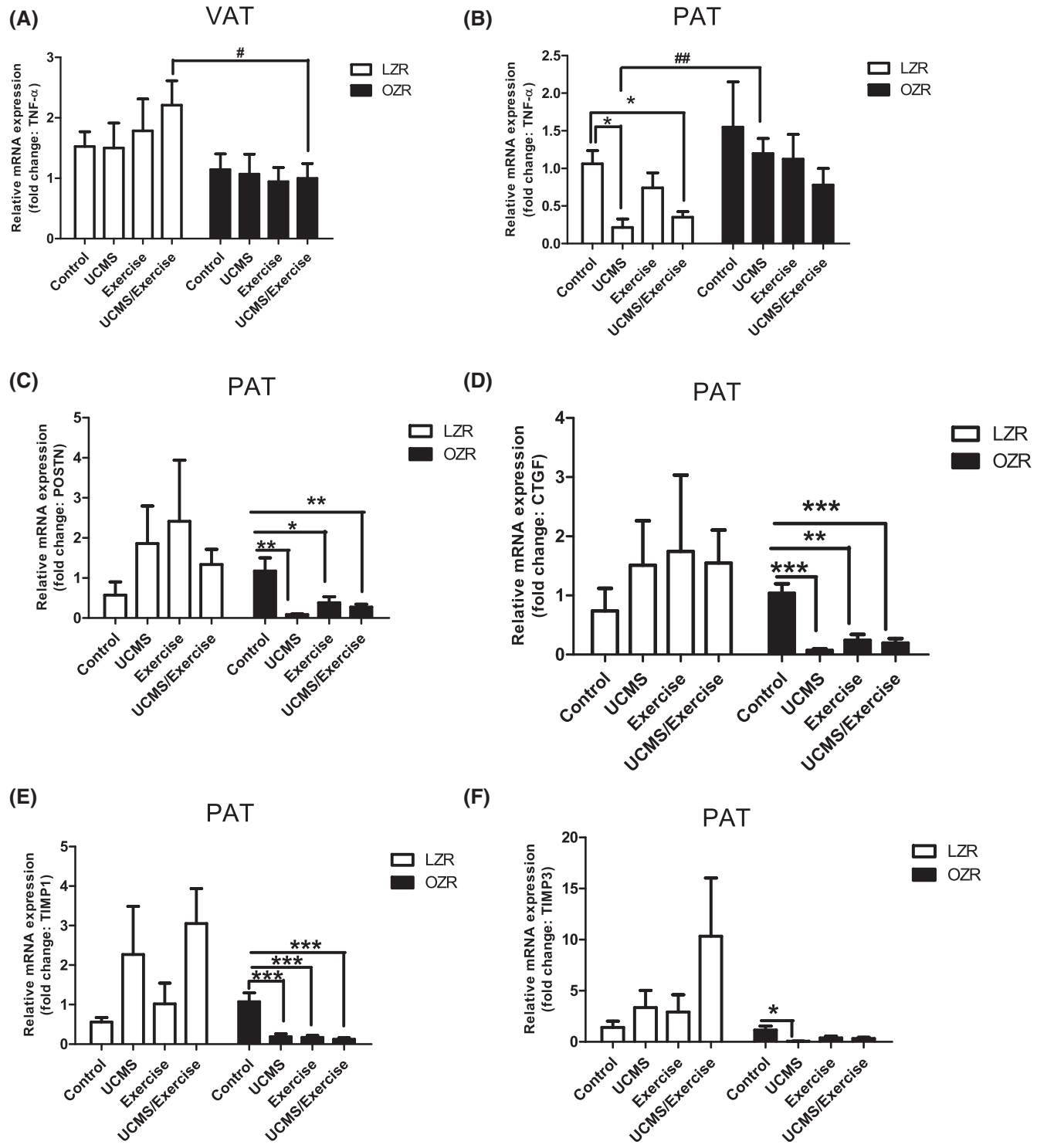

unilocular white adipocytes that expand via hypertrophy, a study demonstrated that the number of lipid droplets in brown adipocyte increases significantly in obesity.[69] The increased lipid droplets coalesced, while collagen fibrils were accumulated in the extracellular space around the whitened brown adipocytes with subsequent brown adipocyte death and macrophage infiltration.[70] In our study, the hypertrophic expansion of the unilocular adipocytes was associated with a decrease in tissue fibrosis. It has been suggested that the expansion of adipose tissue in accommodating excess hyperplastic or hypertrophic adipocytes relies on the high degree of flexibility of the extracellular matrix.[71] Our study showed that PAT is significantly more fibrotic than VAT and may explain why the former is more resistant to significant tissue expansion in obesity. However, we found that the combination of impaired leptin receptor signaling, and psychosocial stress led to decreased tissue fibrosis and subsequent hypertrophic

FIGURE 7 The effects of chronic psychosocial stress and treadmill exercise on inflammatory and fibrotic markers in visceral adipose tissue (VAT) and pericardial adipose tissue (PAT) in LZR and OZR. (A) mRNA expression of TNF-α was measured in VAT obtained from LZR and OZR under control, UCMS, exercise, and UCMS/exercise conditions. Results are presented as fold change in gene expression ± SEM. LZR UCMS/exercise versus OZR UCMS/exercise, $p < .05$, $n = 7–13$. (B) mRNA expression of TNF-α was measured in PAT obtained from LZR and OZR under control, UCMS, exercise, and UCMS/exercise conditions. Results are presented as fold change in gene expression ± SEM. LZR control versus LZR UCMS, $p < .05$, $n = 4–5$; LZR control versus LZR UCMS/exercise, $p < .05$, $n = 5–11$; LZR UCMS/exercise versus OZR UCMS/exercise, $p < .05$, $n = 6–11$. (C) mRNA expression of periostin (POSTN) was measured in PAT obtained from LZR and OZR under control, UCMS, exercise, and UCMS/exercise conditions. Results are presented as fold change in gene expression ± SEM. OZR control versus OZR UCMS, ***$p < .01$, $n = 6–8$; OZR control versus OZR exercise, ***$p < .01$, $n = 4–6$; OZR control versus OZR UCMS/exercise, ***$p < .01$, $n = 5–8$. (D) mRNA expression of connective tissue growth factor (CTGF) was measured in PAT obtained from LZR and OZR under control, UCMS, exercise, and UCMS/exercise conditions. Results are presented as fold change in gene expression ± SEM. OZR control versus OZR UCMS, ***$p < .01$, $n = 6–8$; OZR control versus OZR exercise, ***$p < .01$, $n = 4–6$; OZR control versus OZR UCMS/exercise, ***$p < .01$, $n = 5–8$. (E) mRNA expression of tissue inhibitor of metalloproteinase 1 (TIMP1) was measured in PAT obtained from LZR and OZR under control, UCMS, exercise, and UCMS/exercise conditions. Results are presented as fold change in gene expression ± SEM. OZR control versus OZR UCMS, ***$p < .01$, $n = 6–8$; OZR control versus OZR exercise, ***$p < .01$, $n = 4–6$; OZR control versus OZR UCMS/exercise, ***$p < .01$, $n = 5–8$. (F) mRNA expression of tissue inhibitor of metalloproteinase 3 (TIMP3) was measured in PAT obtained from LZR and OZR under control, UCMS, exercise, and UCMS/exercise conditions. Results are presented as fold change in gene expression ± SEM. OZR control versus OZR UCMS, ***$p < .01$, $n = 6–8$. The statistical differences between LZR and OZR under control, UCMS, exercise, and UCMS/exercise conditions were determined by unpaired *t*-test, and the effects of UCMS and/or exercise were determined by one-way ANOVA followed by a Tukey post hoc test to compare the mean for different groups within the same strain.

expansion of the unilocular adipocytes within the PAT. These changes are likely mediated through the decreased expression of fibrotic and differentiation markers such as POSTN, CTGF, TIMP1, and TIMP3 which we also examined. CTGF appears to be highly expressed in pre-adipocytes[72] where levels correlated with fibrosis in epicardial adipose tissue.[73] POSTN levels on the other hand appear to correlate with tissue inflammation and fibrosis.[74] TIMP1 seems to inhibit adipogenesis suggesting that a reduction would induce tissue remodeling.[75] TIMP3 levels, however, are inversely related to adiposity with higher levels inhibiting adipose tissue differentiation.[76] Our findings suggest that changes in these genes are associated with PAT remodeling and fibrosis, particularly, in response to stress. It has been previously shown that there is an inverse correlation between adipose tissue fibrosis and adipocyte size, suggesting that fibrosis promotes adipocyte hyperplasia to preserve adipocyte function by limiting hypertrophy.[77–79] The distribution of the collagen may also be important since an increase in interstitial or pericellular fibrosis over the course of the development of obesity may decrease extracellular matrix flexibility and tissue plasticity, leading to impaired adipocyte function.[80] Mechanistically, the pathological stress may mediate its effects on PAT through increased levels of glucocorticoids. Previous studies have shown that increased levels of corticosterone in rodents resulted in a decrease in thermogenesis and increased lipid accumulation in brown adipose tissue.[81,82] Taken together, a decrease in adipose tissue fibrosis particularly in PAT should be considered a marker of tissue pathology.

Our study showed contrasting changes in gene expression between VAT and PAT in response to exercise and stress suggesting fundamental differences in tissue remodeling. In the presence of functional leptin signaling, exercise decreased insulin sensitivity in VAT while increasing it in PAT. In contrast, when leptin signaling was disrupted in the OZRs, exercise increased insulin sensitivity in VAT but decreased it in the PAT. These data suggest that leptin signaling can influence insulin sensitivity in response to exercise but the response of PAT and VAT under the same conditions is completely different. Previous work has shown that in brown adipose tissue leptin can influence tissue remodeling through its impact on the growth hormone/insulin-like growth factor I axis is involved in metabolic sensing and control.[83] Likewise, UCMS stress increased the adipogenic marker PPAR-γ in OZR relative to LZR, while in the PAT, stress had the opposite effect. This would suggest that in VAT, some adipogenesis is induced in the absence of leptin receptor signaling, while stress reduced adipogenesis in PAT. The physiological reasons for these differential responses between the two depots are unclear. The reasons are likely to be explained by fundamental differences in cellular composition, with PAT being more brown-like in its composition. Secondly, the location of the depot is also likely to impact remodeling in response to both exercise and psychosocial stress. The proximity of PAT to the heart is likely to expose it to cardiac factors which could impact tissue remodeling in response to these two physiological stimuli. Although PAT in rodents does not make direct physical contact with the heart surface in the same way as epicardial adipose tissue in humans, paracrine factors can be communicated via the pericardial fluid. Bi-directional communication between adipose tissue and muscle has been shown to influence

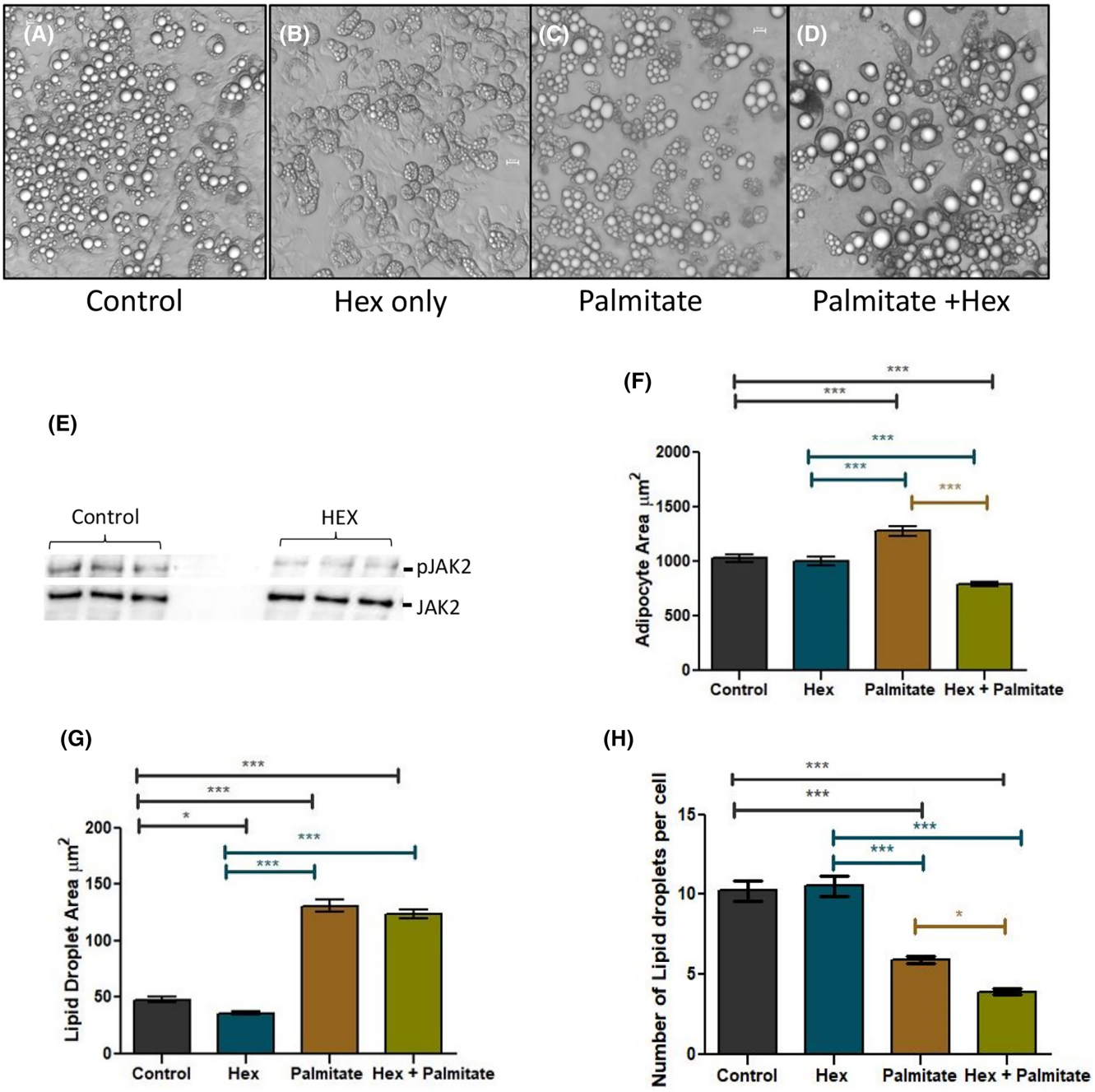

FIGURE 8 Leptin signaling is required for adipocyte cellular hypertrophy but not droplet size. (A) Bright-field images of mature 3T3L1 adipocytes captured at ×40 magnification. Panel A shows untreated control 3T3-L1 mature adipocytes, panel B shows adipocytes that have been treated with 5 µM Hex for 48 h post-maturation. Panel C shows adipocytes treated with 500 µM sodium palmitate for 48 h post-maturation. Panel D shows adipocytes incubated with both palmitate and Hex for 48 h post-maturation. The scale bar in all panels is 20 µm long. Panel E shows a Western blot of control adipocytes and cells treated with 5 µM Hex for 48 h. Panel F shows adipocyte cell area. Panel G shows the average lipid droplet area. Panel H shows the average lipid droplet number per cell in the treatment groups. A total of 100 adipocytes per group were analyzed. Values presented as mean ± SEM, significance was attained at $*p < .01$ and $***p < .0001$, and statistical analysis was done using a one-way ANOVA with a Tukey multiple comparisons test.

both tissue types which has significant implications for metabolic health.[84]

In conclusion, our study shows for the first time that VAT and PAT remodel differently in response to both exercise and psychosocial stress and that these differences are also influenced by leptin receptor signaling (This is shown schematically in Figure 9). In PAT, impaired leptin receptor signaling results in pathological tissue remodeling to both exercise and stress. The role of leptin signaling has been further strengthened by our in vitro

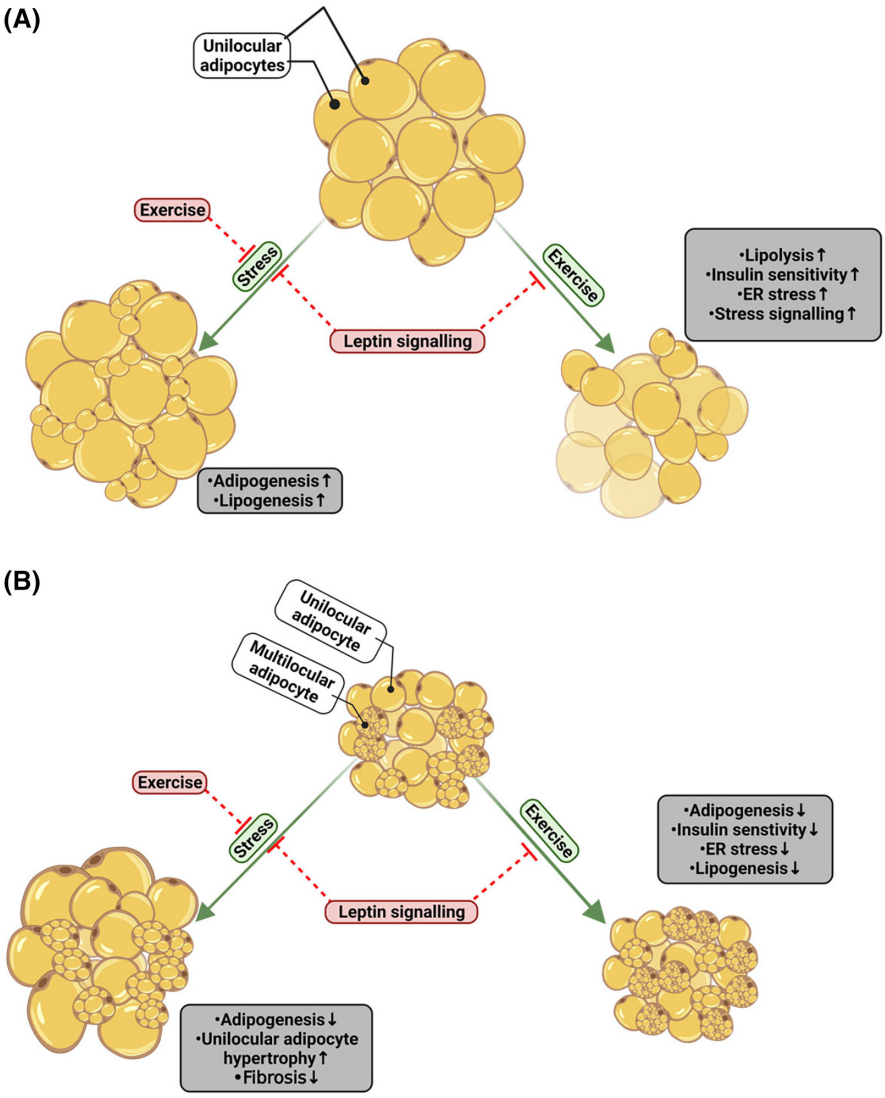

FIGURE 9 Schematic summarizing mechanistically the remodeling of visceral and pericardial adipose tissue with exercise or psychosocial stress in the presence and absence of leptin signaling. Panel A shows the remodeling of visceral adipose tissue with exercise and psychosocial stress and the influence of leptin signaling. Visceral adipose tissue consists of large unilocular adipocytes which increase adipogenesis and lipogenesis in response to psychosocial stress. Exercise induces lipolysis resulting in a reduction in the size of adipocytes. Insulin sensitivity and stress signaling are also increased by exercise. The remodeling is significantly attenuated in the absence of leptin signaling. Panel B shows the remodeling of pericardial adipose tissue with exercise and psychosocial stress and the influence of leptin signaling. Pericardial adipose tissue consists of a mixture of smaller unilocular adipocytes and even smaller multilocular (brown-like) cells. Psychosocial stress, which decreases adipogenesis and tissue fibrosis, is associated with hypertrophy of the unilocular adipocytes. Exercise decreases adipogenesis, lipogenesis, insulin sensitivity, and ER stress. As with visceral adipose tissue, the remodeling is significantly attenuated in the absence of leptin signaling. Image created with Biorender.com

data showing that functional leptin signaling is required for adipocyte cell, but not lipid droplet remodeling in response to hypertrophy stimuli. These data may have significant implications for PAT remodeling in human obesity where leptin receptor signaling is often impaired. In obesity, the remodeling of PAT is likely to have significant implications for cardiac physiology and pathology in response to physiological stimuli such as exercise and psychosocial stress.

AUTHOR CONTRIBUTIONS

Samuel Y. Boateng, Paul Chantler, Dyan Sellayah, Susan Ige, and Mark L. Dallas designed the experiments. Paul Chantler performed the animal experiments, sample collection, and physiological data. Susan Ige, Kaouthar Alaoui, Alaa Al-Dibouni, and Felino R. Cagampang performed the experiments on the tissue samples. Susan Ige, Kaouthar Alaoui, Alaa Al-Dibouni, Mark Dallas, Felino R. Cagampang, Dyan Sellayah, Paul Chantler, and Samuel Y.

Boateng all contributed to the data analysis and/or writing of the manuscript.

ACKNOWLEDGMENTS

The authors would like to thank the Petroleum Technology Development Fund (Abuja, Nigeria) and NIH, NINDS BINP R01 NS117754 for funding this research project.

DISCLOSURES

The authors have nothing to declare regarding any conflicts of interest.

DATA AVAILABILITY STATEMENT

The data that support the findings of this study are available on request from the corresponding author Samuel Y. Boateng.

REFERENCES

1. García-Eguren G, Sala-Vila A, Giró O, Vega-Beyhart A, Hanzu FA. Long-term hypercortisolism induces lipogenesis promoting palmitic acid accumulation and inflammation in visceral adipose tissue compared with HFD-induced obesity. *Am J Physiol Endocrinol Metab*. 2020;318(6):E995-E1003.
2. Wang Y, Yan C, Liu L, et al. 11β-Hydroxysteroid dehydrogenase type 1 shRNA ameliorates glucocorticoid-induced insulin resistance and lipolysis in mouse abdominal adipose tissue. *Am J Physiol Endocrinol Metab*. 2015;308(1):E84-E95.
3. Dube S, Norby BJ, Pattan V, Carter RE, Basu A, Basu R. 11β-hydroxysteroid dehydrogenase types 1 and 2 activity in subcutaneous adipose tissue in humans: implications in obesity and diabetes. *J Clin Endocrinol Metab*. 2015;100(1):E70-E76.
4. Alonso-Alonso M, Pascual-Leone A. The right brain hypothesis for obesity. *JAMA*. 2007;297(16):1819-1822.
5. Ippoliti F, Canitano N, Businaro R. Stress and obesity as risk factors in cardiovascular diseases: a neuroimmune perspective. *J Neuroimmune Pharmacol*. 2013;8(1):212-226.
6. Yi SY, Steffen LM, Terry JG, et al. Added sugar intake is associated with pericardial adipose tissue volume. *Eur J Prev Cardiol*. 2020;27(18):2016-2023.
7. Zsóri G, Illés D, Iványi E, et al. In new-onset diabetes mellitus, metformin reduces fat accumulation in the liver, but not in the pancreas or pericardium. *Metab Syndr Relat Disord*. 2019;17(5):289-295.
8. de Wit-Verheggen VHW, Altintas S, Spee RJM, et al. Pericardial fat and its influence on cardiac diastolic function. *Cardiovasc Diabetol*. 2020;19(1):129.
9. Li SJ, Wu TW, Chien MJ, Mersmann HJ, Chen CY. Involvement of pericardial adipose tissue in cardiac fibrosis of dietary-induced obese minipigs—role of mitochondrial function. *Biochim Biophys Acta Mol Cell Biol Lipids*. 2019;1864(7):957-965.
10. Wang CY, Li SJ, Wu TW, et al. The role of pericardial adipose tissue in the heart of obese minipigs. *Eur J Clin Invest*. 2018;48(7):e12942.
11. Dey D, Wong ND, Tamarappoo B, et al. Computer-aided noncontrast CT-based quantification of pericardial and thoracic fat and their associations with coronary calcium and metabolic syndrome. *Atherosclerosis*. 2010;209(1):136-141.
12. Brinkley TE, Hsu FC, Carr JJ, et al. Pericardial fat is associated with carotid stiffness in the multi-ethnic study of atherosclerosis. *Nutr Metab Cardiovasc Dis*. 2011;21(5):332-338.
13. Elie AG, Jensen PS, Nissen KD, et al. Adipokine imbalance in the pericardial cavity of cardiac and vascular disease patients. *PLoS One*. 2016;11(5):e0154693.
14. Li M, Qi L, Li Y, et al. Association of pericardiac adipose tissue with coronary artery disease. *Front Endocrinol (Lausanne)*. 2021;12:724859.
15. Kim JS, Kim SW, Lee JS, et al. Association of pericardial adipose tissue with left ventricular structure and function: a region-specific effect? *Cardiovasc Diabetol*. 2021;20(1):26.
16. Tang Y, He Y, Li C, et al. RPS3A positively regulates the mitochondrial function of human periaortic adipose tissue and is associated with coronary artery diseases. *Cell Discov*. 2018;4:52.
17. Lau FH, Deo RC, Mowrer G, et al. Pattern specification and immune response transcriptional signatures of pericardial and subcutaneous adipose tissue. *PLoS One*. 2011;6(10):e26092.
18. Kazemi F, Zahediasl S. Effects of exercise training on adipose tissue apelin expression in streptozotocin-nicotinamide induced diabetic rats. *Gene*. 2018;662:97-102.
19. de Sousa Neto IV, Prestes J, Pereira GB, et al. Protective role of intergenerational paternal resistance training on fibrosis, inflammatory profile, and redox status in the adipose tissue of rat offspring fed with a high-fat diet. *Life Sci*. 2022;295:120377.
20. Hausman DB, DiGirolamo M, Bartness TJ, Hausman GJ, Martin RJ. The biology of white adipocyte proliferation. *Obes Rev*. 2001;2(4):239-254.
21. Myers A, Dalton M, Gibbons C, Finlayson G, Blundell J. Structured, aerobic exercise reduces fat mass and is partially compensated through energy intake but not energy expenditure in women. *Physiol Behav*. 2019;199:56-65.
22. Sutherland LN, Bomhof MR, Capozzi LC, Basaraba SAU, Wright DC. Exercise and adrenaline increase PGC-1{alpha} mRNA expression in rat adipose tissue. *J Physiol*. 2009;587(Pt 7):1607-1617.
23. Trevellin E, Scorzeto M, Olivieri M, et al. Exercise training induces mitochondrial biogenesis and glucose uptake in subcutaneous adipose tissue through eNOS-dependent mechanisms. *Diabetes*. 2014;63(8):2800-2811.
24. Hu S, Tucker L, Wu C, Yang L. Beneficial effects of exercise on depression and anxiety during the Covid-19 pandemic: a narrative review. *Front Psych*. 2020;11:587557.
25. Yates BE, DeLetter MC, Parrish EM. Prescribed exercise for the treatment of depression in a college population: an interprofessional approach. *Perspect Psychiatr Care*. 2020;56(4):894-899.
26. Arvidson E, Dahlman AS, Börjesson M, Gullstrand L, Jonsdottir IH. Exercise training and physiological responses to acute stress: study protocol and methodological considerations of a randomised controlled trial. *BMJ Open Sport Exerc Med*. 2018;4(1):e000393.
27. Brooks S, Brnayan KW, DeVallance E, et al. Psychological stress-induced cerebrovascular dysfunction: the role of metabolic syndrome and exercise. *Exp Physiol*. 2018;103(5):761-776.
28. Willner P. Validity, reliability and utility of the chronic mild stress model of depression: a 10-year review and evaluation. *Psychopharmacology (Berl)*. 1997;134(4):319-329.
29. Mineur YS, Belzung C, Crusio WE. Functional implications of decreases in neurogenesis following chronic mild stress in mice. *Neuroscience*. 2007;150(2):251-259.

30. Toni LS, Garcia AM, Jeffrey DA, et al. Optimization of phenol-chloroform RNA extraction. *MethodsX*. 2018;5:599-608.
31. Hansson B, Wasserstrom S, Morén B, et al. Intact glucose uptake despite deteriorating signaling in adipocytes with high-fat feeding. *J Mol Endocrinol*. 2018;60(3):199-211.
32. Hansson B, Morén B, Fryklund C, et al. Adipose cell size changes are associated with a drastic actin remodeling. *Sci Rep*. 2019;9(1):12941.
33. Poret JM, Souza-Smith F, Marcell SJ, et al. High fat diet consumption differentially affects adipose tissue inflammation and adipocyte size in obesity-prone and obesity-resistant rats. *Int J Obes (Lond)*. 2018;42(3):535-541.
34. Jacobs SAH, Gart E, Vreeken D, et al. Sex-specific differences in fat storage, development of non-alcoholic fatty liver disease and brain structure in juvenile HFD-induced obese Ldlr−/−.Leiden mice. *Nutrients*. 2019;11(8):1861.
35. Galinier A, Carriere A, Fernandez Y, et al. Site specific changes of redox metabolism in adipose tissue of obese Zucker rats. *FEBS Lett*. 2006;580(27):6391-6398.
36. Liu A, Sonmez A, Yee G, et al. Differential adipogenic and inflammatory properties of small adipocytes in Zucker obese and lean rats. *Diab Vasc Dis Res*. 2010;7(4):311-318.
37. Iannitti T, Graham A, Dolan S. Increased central and peripheral inflammation and inflammatory hyperalgesia in Zucker rat model of leptin receptor deficiency and genetic obesity. *Exp Physiol*. 2012;97(11):1236-1245.
38. DeVallance ER, Branyan KW, Olfert IM, et al. Chronic stress induced perivascular adipose tissue impairment of aortic function and the therapeutic effect of exercise. *Exp Physiol*. 2021;106(6):1343-1358.
39. Wang J, Ge J, Cao H, et al. Leptin promotes white adipocyte browning by inhibiting the Hh signaling pathway. *Cells*. 2019;8(4):372.
40. Yam KY, Naninck EFG, Abbink MR, et al. Exposure to chronic early-life stress lastingly alters the adipose tissue, the leptin system and changes the vulnerability to western-style diet later in life in mice. *Psychoneuroendocrinology*. 2017;77:186-195.
41. Delker E, AlYami B, Gallo LC, Ruiz JM, Szklo M, Allison MA. Chronic stress burden, visceral adipose tissue, and adiposity-related inflammation: the multi-ethnic study of atherosclerosis. *Psychosom Med*. 2021;83(8):834-842.
42. McCarty R, Horwatt K, Konarska M. Chronic stress and sympathetic-adrenal medullary responsiveness. *Soc Sci Med*. 1988;26(3):333-341.
43. Warne JP. Shaping the stress response: interplay of palatable food choices, glucocorticoids, insulin and abdominal obesity. *Mol Cell Endocrinol*. 2009;300(1–2):137-146.
44. Michel C, Duclos M, Cabanac M, Richard D. Chronic stress reduces body fat content in both obesity-prone and obesity-resistant strains of mice. *Horm Behav*. 2005;48(2):172-179.
45. Reich CG, Taylor ME, McCarthy MM. Differential effects of chronic unpredictable stress on hippocampal CB1 receptors in male and female rats. *Behav Brain Res*. 2009;203(2):264-269.
46. Harris RB, Zhou J, Youngblood BD, Smagin GN, Ryan DH. Failure to change exploration or saccharin preference in rats exposed to chronic mild stress. *Physiol Behav*. 1997;63(1):91-100.
47. Nieuwenhuizen AG, Rutters F. The hypothalamic-pituitary-adrenal-axis in the regulation of energy balance. *Physiol Behav*. 2008;94(2):169-177.
48. Kivimaki M, Head J, Ferrie JE, et al. Work stress, weight gain and weight loss: evidence for bidirectional effects of job strain on body mass index in the Whitehall II study. *Int J Obes (Lond)*. 2006;30(6):982-987.
49. Block JP, He Y, Zaslavsky AM, Ding L, Ayanian JZ. Psychosocial stress and change in weight among US adults. *Am J Epidemiol*. 2009;170(2):181-192.
50. Nyberg ST, Heikkilä K, Fransson EI, et al. Job strain in relation to body mass index: pooled analysis of 160 000 adults from 13 cohort studies. *J Intern Med*. 2012;272(1):65-73.
51. Tomiyama AJ, Schamarek I, Lustig RH, et al. Leptin concentrations in response to acute stress predict subsequent intake of comfort foods. *Physiol Behav*. 2012;107(1):34-39.
52. Macedo DM, Diez-Garcia RW. Sweet craving and ghrelin and leptin levels in women during stress. *Appetite*. 2014;80:264-270.
53. Kokkinos P. Physical activity, health benefits, and mortality risk. *ISRN Cardiol*. 2012;2012:718789.
54. Wang Y, Xu D. Effects of aerobic exercise on lipids and lipoproteins. *Lipids Health Dis*. 2017;16(1):132.
55. Stinkens R, Brouwers B, Jocken JW, et al. Exercise training-induced effects on the abdominal subcutaneous adipose tissue phenotype in humans with obesity. *J Appl Physiol (1985)*. 2018;125(5):1585-1593.
56. Otero-Díaz B, Rodríguez-Flores M, Sánchez-Muñoz V, et al. Exercise induces white adipose tissue browning across the weight spectrum in humans. *Front Physiol*. 2018;9:1781.
57. Jenkins NT, Hagberg JM. Aerobic training effects on glucose tolerance in prediabetic and normoglycemic humans. *Med Sci Sports Exerc*. 2011;43(12):2231-2240.
58. Büsing F, Hägele FA, Nas A, Hasler M, Müller MJ, Bosy-Westphal A. Impact of energy turnover on the regulation of glucose homeostasis in healthy subjects. *Nutr Diabetes*. 2019;9(1):22.
59. Sothmann MS, Buckworth J, Claytor RP, Cox RH, White-Welkley JE, Dishman RK. Exercise training and the cross-stressor adaptation hypothesis. *Exerc Sport Sci Rev*. 1996;24:267-287.
60. Stanford KI, Middelbeek RJ, Goodyear LJ. Exercise effects on white adipose tissue: beiging and metabolic adaptations. *Diabetes*. 2015;64(7):2361-2368.
61. Magkos F, Mohammed BS, Patterson BW, Mittendorfer B. Free fatty acid kinetics in the late phase of postexercise recovery: importance of resting fatty acid metabolism and exercise-induced energy deficit. *Metabolism*. 2009;58(9):1248-1255.
62. Herd SL, Kiens B, Boobis LH, Hardman AE. Moderate exercise, postprandial lipemia, and skeletal muscle lipoprotein lipase activity. *Metabolism*. 2001;50(7):756-762.
63. Gill JM, Frayn KN, Wootton SA, Miller GJ, Hardman AE. Effects of prior moderate exercise on exogenous and endogenous lipid metabolism and plasma factor VII activity. *Clin Sci (Lond)*. 2001;100(5):517-527.
64. Gill JM, Al-Mamari A, Ferrell WR, et al. Effects of prior moderate exercise on postprandial metabolism and vascular function in lean and centrally obese men. *J Am Coll Cardiol*. 2004;44(12):2375-2382.
65. Peng H, Mu P, Li H, et al. Caveolin-1 is essential for the improvement of insulin sensitivity through AKT activation during glargine treatment on diabetic mice. *J Diabetes Res*. 2021;2021:9943344.
66. Karagiannides I, Golovatscka V, Bakirtzi K, et al. Chronic unpredictable stress regulates visceral adipocyte-mediated glucose

metabolism and inflammatory circuits in male rats. *Physiol Rep*. 2014;2(5):e00284.
67. Mahabadi AA, Massaro JM, Rosito GA, et al. Association of pericardial fat, intrathoracic fat, and visceral abdominal fat with cardiovascular disease burden: the Framingham heart study. *Eur Heart J*. 2009;30(7):850-856.
68. Ueda Y, Shiga Y, Idemoto Y, et al. Association between the presence or severity of coronary artery disease and pericardial fat, paracardial fat, epicardial fat, visceral fat, and subcutaneous fat as assessed by multi-detector row computed tomography. *Int Heart J*. 2018;59(4):695-704.
69. Majka Z, Czamara K, Janus J, Kępczyński M, Kaczor A. Prominent hypertrophy of perivascular adipocytes due to short-term high fat diet. *Biochim Biophys Acta Mol Basis Dis*. 2022;1868(2):166315.
70. Kotzbeck P, Giordano A, Mondini E, et al. Brown adipose tissue whitening leads to brown adipocyte death and adipose tissue inflammation. *J Lipid Res*. 2018;59(5):784-794.
71. Rutkowski JM, Stern JH, Scherer PE. The cell biology of fat expansion. *J Cell Biol*. 2015;208(5):501-512.
72. Yoshino J, Patterson BW, Klein S. Adipose tissue CTGF expression is associated with adiposity and insulin resistance in humans. *Obesity (Silver Spring)*. 2019;27(6):957-962.
73. Wang Q, Xi W, Yin L, et al. Human epicardial adipose tissue cTGF expression is an independent risk factor for atrial fibrillation and highly associated with atrial fibrosis. *Sci Rep*. 2018;8(1):3585.
74. Nakazeki F, Nishiga M, Horie T, et al. Loss of periostin ameliorates adipose tissue inflammation and fibrosis in vivo. *Sci Rep*. 2018;8(1):8553.
75. Meissburger B, Stachorski L, Röder E, Rudofsky G, Wolfrum C. Tissue inhibitor of matrix metalloproteinase 1 (TIMP1) controls adipogenesis in obesity in mice and in humans. *Diabetologia*. 2011;54(6):1468-1479.
76. Bernot D, Barruet E, Poggi M, Bonardo B, Alessi MC, Peiretti F. Down-regulation of tissue inhibitor of metalloproteinase-3 (TIMP-3) expression is necessary for adipocyte differentiation. *J Biol Chem*. 2010;285(9):6508-6514.
77. Divoux A, Tordjman J, Lacasa D, et al. Fibrosis in human adipose tissue: composition, distribution, and link with lipid metabolism and fat mass loss. *Diabetes*. 2010;59(11):2817-2825.
78. Michaud A, Tordjman J, Pelletier M, et al. Relevance of omental pericellular adipose tissue collagen in the pathophysiology of human abdominal obesity and related cardiometabolic risk. *Int J Obes (Lond)*. 2016;40(12):1823-1831.
79. Muir LA, Neeley CK, Meyer KA, et al. Adipose tissue fibrosis, hypertrophy, and hyperplasia: correlations with diabetes in human obesity. *Obesity (Silver Spring)*. 2016;24(3):597-605.
80. Sun K, Tordjman J, Clément K, Scherer PE. Fibrosis and adipose tissue dysfunction. *Cell Metab*. 2013;18(4):470-477.
81. van den Beukel JC, Boon MR, Steenbergen J, et al. Cold exposure partially corrects disturbances in lipid metabolism in a male mouse model of glucocorticoid excess. *Endocrinology*. 2015;156(11):4115-4128.
82. Kaikaew K, Steenbergen J, van Dijk TH, Grefhorst A, Visser JA. Sex difference in corticosterone-induced insulin resistance in mice. *Endocrinology*. 2019;160(10):2367-2387.
83. Barrios V, Frago LM, Canelles S, et al. Leptin modulates the response of Brown adipose tissue to negative energy balance: implication of the GH/IGF-I Axis. *Int J Mol Sci*. 2021;22(6):2827.
84. Leal LG, Lopes MA, Batista ML Jr. Physical exercise-induced Myokines and muscle-adipose tissue crosstalk: a review of current knowledge and the implications for health and metabolic diseases. *Front Physiol*. 2018;9:1307.

SUPPORTING INFORMATION

Additional supporting information can be found online in the Supporting Information section at the end of this article.

How to cite this article: Ige S, Alaoui K, Al-Dibouni A, et al. Leptin-dependent differential remodeling of visceral and pericardial adipose tissue following chronic exercise and psychosocial stress. *The FASEB Journal*. 2023;38:e23325. doi:10.1096/fj.202300269RRR